2017

Examination of the Potential of Structure-from-Motion Photogrammetry and Terrestrial Laser Scanning for Rapid Nondestructive Field Measurement of Grass Biomass

Sam D. Cooper
South Dakota State University

EXAMINATION OF THE POTENTIAL OF STRUCTURE-FROM-MOTION PHOTOGRAMMETRY AND TERRESTRIAL LASER SCANNING FOR RAPID NONDESTRUCTIVE FIELD MEASUREMENT OF GRASS BIOMASS

BY

SAM D. COOPER

A thesis submitted in partial fulfillment of the requirements for the

Master of Science

Major in Geography

South Dakota State University

2017

EXAMINATION OF THE POTENTIAL OF STRUCTURE-FROM-MOTION PHOTOGRAMMETRY AND TERRESTRIAL LASER SCANNING FOR RAPID NONDESTRUCTIVE FIELD MEASUREMENT OF GRASS BIOMASS

SAM D. COOPER

This thesis is approved as a creditable and independent investigation by a candidate for the Master of Science in Geography degree and is acceptable for meeting the thesis requirements for this degree. Acceptance of this does not imply that the conclusions reached by the candidate are necessarily the conclusions of the major department.

David Roy, Ph.D.
Thesis Advisor Date

George White, Ph.D.
Head, Department of Geography Date

Dean, Graduate School Date

ACKNOWLEDGEMENTS

First and foremost I would like to thank my advisor Dr. David Roy without whom none of this would be possible. His guidance throughout this project was invaluable, and he has pushed me to grow as a researcher and always strive for the best.

This research was funded by a South Dakota State University (SDSU) Geospatial Sciences Center of Excellence Research Assistantship, and I would like to thank the Center for providing me with the resources needed to conduct this project. Thanks also goes to the SDSU Geography Department faculty for their guidance and support. Thanks especially to Dr. Sanath Sathyachandran, for providing me with advice in the formative stages of this project and assistance conducting field work.

I would also like to thank Dr. Crystal Schaaf and her lab at the University of Massachusetts Boston for their work in developing the Compact Biomass LiDAR, and in particular Francesco Peri for his technical expertise and assistance. Many thanks go to Dr. Nels Troelstrup and the Oak Lake Field Station for access to the field station for field work and destructive sampling without which this project would not have been possible, as well as Dr. Xu Lan for the use of her lab and Dr. Sandy Smart for guidance with disc pasture meter selection and construction.

A special thanks especially goes to my Committee: Dr. Xiaoyang Zhang, Dr. Yan Lin, and Dr. Robin Brown.

Finally, I would like to thank my all of my friends and family, for their support and encouragement throughout.

CONTENTS

ABBREVIATIONS

AGB	Aboveground Biomass
CBL	Compact Biomass LiDAR
DBH	Diameter at Breast Height
DEM	Digital Elevation Model
DSLR	Digital single-lens reflex
LiDAR	Light detection and ranging
LOOCV	Leave-one-out Cross Validation
OLS	Ordinary Least Squares
RMA	Reduced Major Axis
RMSE	Root Mean Squared Error
SfM	Structure-from-Motion
TLS	Terrestrial Laser Scanning

LIST OF FIGURES

LIST OF TABLES

ABSTRACT

EXAMINATION OF THE POTENTIAL OF STRUCTURE-FROM-MOTION PHOTOGRAMMETRY AND TERRESTRIAL LASER SCANNING FOR RAPID NONDESTRUCTIVE FIELD MEASUREMENT OF GRASS BIOMASS

SAM D. COOPER

2017

Above ground biomass (AGB) is a parameter commonly used for assessment of grassland systems. While destructive sampling of AGB is highly accurate, it is time consuming and often precludes repeat temporal sampling or sampling in sensitive ecosystems. Consequently, a number of nondestructive techniques that relate grass structural properties to AGB have been developed. This study investigated the application of two recent technologies, Terrestrial Laser Scanning (TLS) and Structure-from-Motion (SfM), in the development of rapid nondestructive AGB estimation of grassland plots. TLS and SfM volume metrics generated using a rasterized surface differencing method were linearly related to destructively measured total AGB and grass AGB excluding all litter, and results were compared to the conventional disc pasture meter. The linear models were assessed using a leave-one-out cross validation scheme. The disc pasture meter was found to be the least reliable method in assessing total AGB (r^2 = 0.32, $RMSE_{LOOCV}$ = 269 g/m2). SfM (r^2 = 0.74, $RMSE_{LOOCV}$ = 169 g/m2) outperformed TLS (r^2 = 0.56, $RMSE_{LOOCV}$ = 219 g/m^2), though a much larger slope in SfM regressions suggests an increased sensitivity to error. Litter removal decreased the effectiveness of AGB estimation for both TLS (r^2 = 0.49) and SfM (r^2 = 0.51) but increased the fit of disc pasture meter estimations (r^2 = 0.42), highlighting the complex

relationship between litter accumulation and AGB. TLS and SfM derived volumes were shown to be insensitive to cell dimensions when calculating volume provided cell dimensions were large enough to ensure no empty cells occurred. Using observed ground surfaces in volumetric calculations rather than an estimated ground plane increased r^2 to 0.63 for TLS and 0.77 for SfM. Though the disc pasture meter was found to be the most rapid of the three methods, TLS and SfM both out performed it and have clearly demonstrated their potential utility for AGB estimation of grass systems. Their ability to systematically collect measurements over larger spatial extents than those investigated here could greatly outpace the disc pasture meter's predictive capabilities and speed.

Keywords: Terrestrial Laser Scanning, Structure-from-Motion, disc pasture meter, grass, aboveground biomass,

1.0 INTRODUCTION

Grasslands and rangelands make up 47% global terrestrial surface area and are home to a wide variety of unique plant and animal species (Owensby et al. 1993). Grasslands directly and indirectly benefit human life around the world through collective benefits known as ecosystem services (Costanza et al. 1997). In grasslands, ecosystems services include basic functions such as food production, wildlife habitat, or waste assimilation, as well as more intangible services such as aesthetic value or cultural significance. Globally, all ecosystem services have been estimated to provide US$ 16 – 54 trillion of unaccounted for value into our economy (Costanza et al. 1997), with grasslands contributing significantly to erosion control, soil formation, and greenhouse gas regulation. Understanding and quantifying the value of ecosystems around the world is the best means to garner larger support for their protection, and accomplishing that requires comprehensive understanding of their health and productivity.

Though the overall productivity of grasslands is proportionally much lower than other ecosystems (e.g., forests), grasslands still are highly productive ecosystems with a large carbon storage capacity and contain up to 30% of the world's soil carbon stock (Scurlock and Hall 1998). Because of low soil turnover, tallgrass ecosystems in particular are important means for long term carbon storage globally (Knapp and Smith 2001).

Measuring and monitoring ecosystem health and suitability is a challenge that is present around the world. A wide range of different indicators have been developed to monitor and understand ecosystems and the drivers that impact them. These indicators vary depending on the ecosystem and lifeforms being assessed. Often, they involve

community species assessment or in depth observations of sensitive or ecologically important species. These processes, however, can be time consuming and require extensive *in situ* study on small spatial scales.

Aboveground biomass (AGB) is one indicator frequently used for ecosystem assessment. It is defined as the weight per unit area of plant material protruding above the soil surface and includes all living vegetation above the soil (Eisfelder et al. 2012). AGB is therefore closely related to ecosystem net primary production (NPP), which can be measured as the amount of organic matter (i.e. vegetation) produced per unit area in a given time. This is not only a fundamental aspect to all life on earth, but it also plays an important role in global carbon cycling, a process of great importance to the study of climate change. AGB is an important metric often used in climate modeling as well as a measure of vegetation production, quality of habitat, and an ecosystem's direct and indirect economic outputs. In grasslands, quantification of AGB is an important tool for a number of applications, including pasture management (Trotter et al. 2010), wildlife habitat monitoring (Carlyle et al. 2010; McNaughton 1985), fire management (Kauffman et al. 1994; Trollope et al. 1996), carbon storage (Scurlock and Hall 1998; Tilman et al. 2006), and understanding the implications of and biophysical and ecological processes that influence grass production (Tilman et al. 2001; Loreau and Hector 2001).

Measuring and monitoring AGB can be quite challenging, and techniques for doing so vary depending on the vegetation under investigation. Direct destructive sampling of AGB involves cutting, drying and weighing all vegetation above the soil surface. It is the most direct and accurate method for AGB measurement, however it is time consuming and highly intrusive by nature (Mannetje 2000). The need to physically

remove vegetation for measurement can further limit site selection and makes repeat sampling difficult if not impossible. The consequence of this is that while higher accuracy in plot measurements may be obtained, studies relying solely on destructive techniques are often limited to fewer plots which could lead to lower site-wide AGB estimation accuracy.

To mitigate this, nondestructive methods have been developed to estimate AGB in grasslands. These methods typically generate allometric relationships between a subset of destructively sampled plots to some structural property (e.g., height and cover Williamson et al. 1987) that can be nondestructively measured across the study site, thereby reducing the need for destructive sampling. These relationships can further be calibrated to specific species composition and site conditions so that allometric calibration through destructive sampling can be bypassed altogether if the correct conditions are met (Zambatis et al. 2006). The use of allometric relationships for AGB estimation has the benefit of leaving a majority of the vegetation intact, but at the cost of lower accuracy. However this allows for more rapid sampling, meaning that a greater number of plots can be assessed in a limited time frame. Given the time constraints many studies face, this could potentially allow for greater site-wide accuracy.

One conventional allometric method commonly used in AGB estimation of grasslands is the disc pasture meter, which allometrically relates the settling height of a weighted disc on a grassland plot to the AGB beneath it (Holmes 1974; Santillan et al. 1979). While the disc pasture meter is rapid and reasonably accurate, it has shown to be less reliable in tall grasses and heterogeneous plots (Santillan et al. 1979; Mannetje 2000; Douglass and Crawford 1994) as well as in the presence of a large litter layer or variable

microtopography across the study site (Karl and Nicholson 1987). Shortcomings such as these in allometric estimation of AGB leave the possibility open for the development of new methodologies in AGB estimation, and recent technological advances in active and passive remote sensing have the potential for rapid nondestructive estimation of grassland AGB.

Two such advances are found in Terrestrial Laser Scanning (TLS) and Structure-from-Motion (SfM) photogrammetry. TLS utilizes Light Detection and Ranging (LiDAR) technology to make three dimensional measurements of an object. These systems require very little training to use and may be deployed rapidly and systematically to return precise and consistent measurements of grassland vegetation. Advances in LiDAR technology have lowered the instrument costs and increased data quality to the point that widespread adoption of the technology is becoming increasingly feasible. The Compact Biomass Lidar (CBL) is one such advance making TLS technologies practical for implementation in a wide array of ecological surveys. The CBL unit is lightweight, portable, and fast scanning, making it a highly versatile instrument allowing for rapid data acquisition (Paynter et al. 2016). Advances such as these have led to the increasing use of TLS systems in vegetation assessment, though most studies have focused on woody vegetation.

Structure-from-Motion (SfM) photogrammetry is a passive remote sensing technology with high potential for vegetation assessment. SfM is a computer vision technique that generates a 3D point cloud similar to that of LiDAR (Nouwakpo et al. 2015). First introduced in 1979 (Ullman 1979), it has only been with recent advances in computing that SfM has become a viable tool for general application. Unlike LiDAR,

which is an active remote sensing technology, SfM point clouds are calculated from a series of overlapping digital photographs. The use of ordinary cameras in SfM data acquisition significantly lowers equipment costs compared to TLS, but like TLS, SfM can be quickly and easily implemented, as users need only know the basics of camera operation and photo capture. While this technology has been successfully implanted in woody vegetation assessments, few studies have explored its utility in assessing herbaceous vegetation such as grasses.

Both TLS and SfM have been shown to be highly effective in woody vegetation assessment and AGB estimation. The implementation of TLS in herbaceous vegetation assessment has been increasing, but direct applications linking TLS measurements to grass AGB estimations remain limited, and SfM remains largely untested in herbaceous systems. Both technologies are being actively explored, however, and no standardized methods of their application have been developed, particularly in grassland systems.

2.0 THESIS OBJECTIVES

This thesis investigates the efficacy of Terrestrial Laser Scanning (TLS) and Structure-from-Motion (SfM) in deriving above ground biomass (AGB) of grassland plots in order to establish new and more efficient means of AGB estimation for grassland ecosystems. To accomplish this, I will address the following questions. For the same prairie grassland system: (1) How accurately can the SfM approach estimate aboveground grass biomass? (2) How accurately can the TLS approach estimate aboveground grass biomass? (3) Are the remote sensing approaches (SfM and TLS) more accurate than the conventional disc pasture meter approach? (4) What are the limitations of each method (TLS, SfM, and disc pasture meter) for rapid field based assessments of aboveground grass biomass?

3.0 A REVIEW OF FIELD BASED METHODS FOR MEASURING ABOVEGROUND BIOMASS

The AGB of grassland systems can be measured in a variety of different ways. Here I present a literature review of conventional field based methods for measuring AGB as well as general application of TLS and SfM technologies in vegetation assessment. Grasslands and rangelands often contain a variety of woody plant species ranging from small shrubs to large trees and can make significant contributions to the AGB of a grassland system. For the purposes of this study, site selection precluded the presence of woody biomass. Nevertheless, woody biomass of various sizes is often present in grassland environments and must be considered when assessing AGB of a grassland system as a whole. Additionally, application of TLS and SfM for vegetation assessment has largely focused on woody vegetation assessment, and application in herbaceous systems has been limited, especially for SfM. Techniques developed for woody vegetation assessment could therefore provide much needed insight into possible applications in a grassland ecosystem. For these reasons, a review of woody vegetation assessment is included in this literature review.

3.1 Conventional Field Based AGB Estimates

Conventional methods for AGB measurement can be grouped into two broad categories: destructive and nondestructive. Destructive techniques are widely regarded as the more accurate of the two, but they have several disadvantages (Mannetje 2000). They are often far more labor intensive than nondestructive techniques. Given that many studies are often limited both in time at resources, this means that while higher accuracy may be obtained, studies utilizing destructive techniques are often limited to fewer sites.

This can be detrimental to large area studies. Furthermore, the removal of vegetation required for destructive sampling means that repeat sampling of a plot is impossible, limiting its use in sites within sensitive ecosystems or some studies of change over time. Consequently, non-destructive techniques requiring less time and obtaining more accurate results are a topic of research.

3.1.1 Field Based AGB Estimates of Grasses

3.1.1.1 Destructive Sampling. For grassland systems, destructive sampling of AGB involves cutting and weighing all vegetation growing above the soil level in a plot. Grasses can be cut either by hand or by machine-driven devices such as specialized harvesters or lawn mowers. The height at which the plot is cut is crucial to obtaining accurate AGB estimates, with consistency being key. The ideal clipping height varies by the community makeup, but typically cutting heights should be low enough to sample a majority of the biomass without accidentally collecting any soil in the sample. After removing the vegetation, samples are typically dried and weighed to obtain the dry matter yield of the sample. While the wet weight of the plant matter may be useful for generalized comparisons, drying is necessary due to the highly variable water content that may exist between the plants being weighed (Mannetje 2000). Prior to drying, the samples can also be sorted by various factors to determine percent composition by species or dead standing versus live standing biomass.

The need for faster and less intrusive measurements has led to the development of many non-destructive methods for AGB estimation specific to grassland communities. These techniques are typically calibrated using a process known as double sampling, in which the destructive sampling of a few plots in a given community is used to establish

allometric relationships between the non-destructive techniques measured at larger spatial extents and the direct AGB measurements. This allows for more rapid AGB estimations of large-scale projects. Non-destructive techniques in grass dominated systems have been grouped into three categories by Mannetje (2000): visual estimation, height and density measurements, and measurements of other attributes related to biomass.

3.1.1.2 Direct Visual Estimation. Direct visual estimation has limited use in scientific research, as researchers simply visually compare plots to a destructively measured reference. However, this method has been shown to sometimes yield accurate results, with a correlation coefficient between estimated and clipped AGB measurements of 0.98 using the comparative yield method developed by Haydock and Shaw (1975). This method involves clipping and weighing a small subset of a plot, and using that subset as a visual reference to estimate the AGB of the entire plot. Boyda (2013) investigated the accuracy of a similar reference unit method in tallgrass prairies, obtaining highly accurate results (r^2 = 0.91). He emphasized a high degree of consistency between different observers in the project, but as data was collected from only three individuals training, consistency between observers in widespread application may be an issue.

Visual obstruction measurement have also been shown to be highly correlative (r^2 = 0.97) to the weight of clipped vegetation (Robel et al. 1970). In this technique, an observer estimates the amount of vegetation obstructed along a transect by recording the lowest observable point at various distances and from different heights. This distance metric can then be allometrically related to AGB of the plot.

3.1.1.3 Height and Density Measurements. Height and density measurements have been found to show strong correlation with aboveground biomass. Reppert et al. (1962) were able to show correlations between vegetation height and percent ground cover using point frame measurements for plant heights and visual estimations of ground cover. While they found individually these metrics were poor indicators of total AGB, combining height, cover, and height multiplied by cover together accounted for 84% of the variation of the vegetation AGB. Williamson et al. (1987) improved upon this relation somewhat by using basal cover and blade length of a plot to estimate AGB (r^2 = 0.87). This relationship was also noted to vary seasonally.

Due to their portability and consistency, disc pasture meters are a widely used tool for AGB estimation of grasses. A disc pasture meter consists of a circular or rectangular plate that slides along a pole and is dropped from a fixed height or lowered gently onto the grass canopy. The height at which it comes to rest is assumed to be a function of the height and density of the grass beneath it and can be allometrically related to the AGB of the plot (Holmes 1974). This method is highly dependent on the grass species composition, phenology, and moisture content of the vegetation. Bransby et al. (1977) tested the effect of varying the disc size and weight on measurements, comparing discs of equal weight per area but different size as well as discs of constant size but differing weights. They found no significant differences in calibration from altered size or weight. This was contrasted by Santillan et al. (1979), who observed higher precision with larger disc sizes. They concluded that this was due to larger discs measuring a greater area of vegetation, thus incorporating a larger degree of plot variability in the measurements.

However, improvements were only slight and they observed that the ease of use of the smaller discs as well as their uniformity across grass species offset their lower precision.

Several different methods for obtaining the AGB measurements from disc pasture meters have been developed. Holmes (1974) pioneered the disc pasture meter technique and allowed the disc to drop from a fixed height. Santillan et al. (1979) found that gently lowering the disc on top of the vegetation reduced variation caused from dropping the disc. Harmoney et al. (1997) found that by allowing the disc to rise slowly as the pole is inserted into the plot, a tighter relationship between resting height and AGB could be achieved. While all of these studies showed strong correlations between disc height and measured AGB, they noted that the disc method appears to be most accurate in homogenous plots. Grassland plots with numerous different species as well as forbs and woody shrubs make this method less effective (Mannetje 2000).

Pasture meters are a relatively new technology that allow for rapid measurement of grass height that can then be allometrically related to AGB. These meters consist of a vertical row of light beams mounted on a trailer. When driven over a pasture, the grasses will disrupt the beams and the highest beam disrupted indicates the maximum height of the grass at that location. Schori et al. (2015) compared the relative effectiveness of a pasture meter to the rising plate meter method of AGB estimation. They found that the pasture meter yielded higher average measurements of grass height, but regressions estimating biomass yielded similar coefficients of determination, with r^2 of 0.81 for the rising plate meter and 0.77 for the pasture meter. The pasture meter, however, took approximately 1/6 of the time that the rising plate meter took for full field assessment.

3.1.1.4 Other Attributes Related to AGB. The electrical capacitance of grasses and other herbaceous vegetation is much higher than that of woody vegetation and bare ground. Taking advantage of this, Vickery and Nicol (1980) obtained high levels of correlation by calibrating measurements to the mean air capacitance. Like disc pasture meters, capacitance can be affected by a variety of factors such as vegetation water content, species composition, and reproductive stage, suggesting that like other allometric methods, the use of capacitance for AGB estimation is best suited for homogenous plots during the same phenological stage. Serrano et al. (2011) confirmed this assumption and found that accuracy varied significantly between homogenous grass dominated plots (r^2 = 0.90), heterogeneous grass plots (r^2 = 0.87) and legume dominated pastures (r^2 = 0.48).

Various field based optical remote sensing techniques for estimating AGB have also been proposed. These methods relate spectral properties of the vegetation to AGB through the use of spectral reflectance indices (e.g., Normalized Difference Vegetation Index). Trotter et al. (2010) used an active sensor emitting red (650nm) and near infrared (880 nm) to quantify AGB in a grass pasture using the Soil Adjusted Vegetation Index, the Normalized Differenced Vegetation Index, the Nonlinear Vegetation Index, the Modified Nonlinear Vegetation Index, the Simple Ratio, and the Modified Simple Ratio. They found that the Soil Adjusted Vegetation Index had the lowest RMSE of 288 kg/ha, largely due to its compensation of near infrared saturation at high biomass levels. Erdle et al. (2011) compared active sensors, such as those used by Trotter et al. (2010), to a bi-directional passive radiometer and found that all sensors were able to describe AGB and of a wheat field, though this broke down when estimating nitrogen content, and varied

significantly by growth stage of the wheat. They also noted that active sensors had the added benefit of not relying on ambient lighting conditions, allowing for greater flexibility in usage.

3.1.2 Woody Field Based Biomass Estimates

3.1.2.1 Destructive Sampling. Measuring AGB of woody vegetation using destructive techniques follows the same general principles as non-woody sampling and is also considered to be the most accurate means for measuring AGB. First, the whole tree or shrub is cut at ground level or a specified height. Typically, the plant material is sorted into wood, twigs, fruits, and leaves, and each component is dried and weighed separately. A diameter based classification is typically used to distinguish between wood and twigs, for example classifying material greater than 5mm in diameter classified as wood and those less than 5mm classified as twigs (Mannetje 2000).

Another destructive technique for woody vegetation assessment is xylometry, or water displacement of the woody components. This method can been used to obtain highly accurate volumetric measurements of woody vegetation (Özçelik et al. 2008), which along with the wood density relates directly to biomass. By compensating for water weight absorbed by the log, the authors were able to obtain more accurate volumetric estimates than previous destructive methods of drying and weighing. While xylometry doesn't directly measure biomass, it is an effective way to obtain and validate volumetric measurements which can then be allometrically related to biomass. Like non-woody sampling methods, the need for less invasive and less resource intensive methods has led to the development of non-destructive techniques to estimate AGB for trees or shrubs.

Woody plant species vary morphologically, ranging from small shrubs to large trees. These different lifeforms have require different methods of AGB measurement. Therefore, clearly differentiating between these groups of woody vegetation is necessary to fully understand the ecosystem and accurately assess its biomass. This is often done based on organism height and the presence of multiple stems and defined crowns (FAO 2015). While destructive measurements of trees and shrubs are largely the same, this distinction is more important in allometric estimations of AGB, which by definition rely on the intrinsic structure of the organism being studied and its relationship to AGB.

3.1.2.2 Nondestructive Sampling of Trees. For trees, diameter at breast height (DBH) is a commonly used metrics to quickly estimate AGB. Differences in morphological traits between different tree species means that direct comparisons to AGB using only DBH require intensive calibration to different species (Ter-Mikaelian and Korzukhin 1997). However, these estimates are often drawn around the assumption that the trunk is both circular and solid. Nogueira et al. (2006) quantified the overestimations inherent to these assumptions by comparing field measurements to measurements from cross-sectional discs. They found an 11% overestimation from DBH and 30% overestimation from total basal area. This was largely due to non-circular form of the trees, with hollow areas only affecting 0.7% of overestimation. Chave et al. (2005) reported another bias in DBH assumptions, observing that neither the cylindrical nor the conic models for stem shape are appropriate for estimating stem volume as the rate at which the stem tappers is not constant.

Many times, multiple metrics are combined to generate more accurate results. Segura and Kanninen (2005) found that the combination of DBH and total height yielded

the best AGB estimates with an r^2 of 0.87 compared to r^2 values ranging from 0.64 - 0.71 without including height. Chave et al. (2005) in their assessment of various regression models to estimate AGB of tropical forests found that the most important predictors in estimating AGB were trunk diameter, wood specific gravity, total height, and forest type.

3.1.2.3 Nondestructive Sampling of Shrubs. Shrubs, which by definition lack a single main stem (FAO 2015), cannot utilize DBH to estimate AGB. Flombaum and Sala (2007) found strong relationships between vegetation cover and AGB for both shrub and grass dominated plots in an arid ecosystem, obtaining r^2 values of 0.74 for shrubs and 0.86 for grasses. To accomplish this, they used a line-intercept method in which they measured canopy overlap along transects as a surrogate for biomass.

Volumetric measurements have also used to estimate shrub biomass. Usó et al. (1997) used height and diameter of the plant at maximum width to create nonlinear regressions estimating AGB. They used three different volumetric models: circular cylinder, elliptical cylinder, and paraboloid of rotation, founding that all three methods accurately describe the relationship between biomass and shrub volume. Alternatively, Sah et al. (2004), used crown area and shrub height for AGB estimations. They obtained r^2 values ranging from 0.68 to 0.99, and found model performance to be highly dependent upon the species of shrub.

The reference unit method has also been applied to woody biomass estimations. Kirmse and Norton (1985) visually estimated biomass of two shrub species using branches ranging from 7 to 19% of total plant foliage. They were able to obtain r^2 values ranging from 0.890 to 0.985 from 3 observers, with higher values obtained from

reference units accounting for more of the total plant volume. They also tested a dimensional analysis method in which cylindrical volumes were calculated from two diameters (the longest width of the plant and the length perpendicular to the longest) and plant height, obtaining r^2 values of up to 0.937.

3.2 Terrestrial Laser Scanning for Vegetation Assessment

Continuing advances in LiDAR technology have resulted in a relatively recent increase in the usage of Terrestrial Laser Scanning (TLS) for variety of applications from surface geomorphology to structural assessments of forest canopies. Research into the viability of TLS systems for vegetation assessment has been dominated by forested ecosystems, but recent years have seen more studies expanding to new ecosystem types such as shrub lands, marshlands, and agricultural plots. Grasslands, in part due to the difficulty of obtaining accurate scans due to high vegetation density and low structural integrity, have seen comparatively limited application of TLS in vegetation assessment.

3.2.1 TLS Overview

Terrestrial Laser Scanning utilizes Light Detection and Ranging (LiDAR) technology to make three dimensional measurements of an object. To accomplish this, the LiDAR scanner first emits a pulse of light at a set frequency. The pulse is reflected off an object of interest, and the instrument records the amount of time for the return pulse to reach the sensor. The distance from the scanner to the object is then calculated from the travel time of the light pulse and the speed of light through the atmosphere and combined with the angle of the pulse can be used to determine the location of the reflective object. What results is a three dimensional mass of data called a point cloud in

which each point represents the location relative to the sensor of an object that reflected the laser pulse back. The point cloud can be oriented to a single XYZ coordinate system and used to infer structural attributes from the object.

The laser returns themselves can be measured in a few different ways. The most common is for the time of flight and intensity of a discrete number of returns to be recorded. For the purposes of this study, a scanning system in which first and last returns are recorded will be used. Full waveform processing similarly records time of flight pulses, but it is also capable of measuring the entire waveform of the return, allowing for more data to be extracted from a single laser pulse. Phase based scanners act somewhat differently from the other two. They modulate the laser into several phases and use the properties of the phase shifts in the returns to determine the distance to the object.

The LiDAR technology utilized by TLS has already been well established with Airborne Laser Scanning (ALS), which has received significantly more use as a LiDAR platform than TLS, and several methods developed for ALS point cloud interpretation have been successfully applied to interpret TLS derived point clouds. However, TLS offers some significant advantages over ALS in some situations. For example, the low scan angles of TLS systems can help with measurements of low stature vegetation such as shrubs (Vierling et al. 2013). Additionally, TLS can typically provide a much more dense point cloud than ALS, a feature that is crucial for measuring fine scale vegetation such as grasses, and one which may be used to better calibrate ALS data over larger spatial extents (Greaves et al. 2017). This is particularly useful in forested or savanna systems where it can provide accurate understory information that would otherwise be occluded from ALS data by taller vegetation (Loudermilk et al. 2009). The high point

cloud density and ease of implementation of TLS systems compared to ALS campaigns make TLS highly effective for studies of small areas or areas that require repeat surveys. This emphasis on highly detailed scans over a small spatial extent is ideal for plot level surveys such as this project.

3.2.2 TLS for Woody Vegetation Assessment

3.2.2.1 Trees. One of the most well established applications of TLS in regards to vegetation assessment is in forestry. TLS has been used to model AGB as well as various aspects of forest structure. Kankare et al. (2013) developed models for AGB as well as tree stem, living branch, and dead branch biomass, estimated using ratios derived from felled trees. Their models compared well to previously developed models, but greatly outperformed others in branch biomass. Seielstad et al. (2011) modeled biomass of small and large branches by scanning individual branches of different size from different angles and orientations. They established a linear relation between return scan density and biomass (r^2 = 0.898 for small branches and 0.937 for large branches).

Hosoi and Omasa (2006) established a voxel-based method for 3D modeling from which they derived leaf area density and leaf area index of individual trees. This method assigns each return point to a three dimensional box, or 'voxel', the size of which is optimized based on statistical analysis of the point cloud. They found this method to be highly accurate when combined with an optimal scan inclination and it provides several advantages over previous TLS techniques, including the elimination of overlapping points and an intuitive 3D array allowing for straightforward computation. Hosoi and Omasa (2013) were able to use the spatial distribution of voxels derived from their 2006 methodology to distinguish between woody and non-woody biomass in a broad-leaf tree.

More advanced methods of volumetric measurement have been developed that implement quantitative models to generate highly precise stem and branch volumes from TLS point clouds (Raumonen et al. 2013). These operate by locally modeling patches to generate cylinders around regions of the stems and branches and extrapolating these models to neighboring regions to produce a full tree model. Volumes derived from these models can then be related to destructively measured AGB to generate allometric measures of AGB (e.g., Calders et al. 2014). These methods can also be used to assess the structure of trees with exposed buttressed root systems, for example in mangrove ecosystems (Paynter et al. 2016). However, this methodology requires that individual stems be resolved in the point cloud. Given the closed packed nature of grasses and subsequent occlusion of much of the grass stem, applying methods such as these to grasslands may not be possible.

More recently, Grau et al. (2017) used a ray-tracing simulation to calculate the plant area index of simulated trees using a multi-return TLS framework. By using the radiative transfer laws and the estimated number of beams passing through each voxel, the authors were able to assess the internal structure of the canopy. Through extensive sensitivity testing, they found that the main sources of error in their method derived from poor voxel sampling, small voxels relative to leaf size, coarse angular resolutions (θ = 0.5°), and using first-return only TLS systems. When applied to realistic tree models, the authors emphasized the strong effects of vegetation structure and occlusion on the accuracy of the results. The methodologies employed utilized the properties of multi-echo returns, and therefore their findings may not be directly applicable to the current study.

Calders et al. (2014) investigated the relationship between TLS derived vertical plant profiles and topography. Even with relatively flat locations, they found that not correcting for topography can lead to significant errors. The TLS plane fitting approach they outlined reduced error in height measurements by 77-100%. This is based on ALS data acting as the 'truth', which the findings of Zhao et al. (2013) indicates is not always a safe assumption.

Several studies have also compared TLS to other non-destructive allometric models. Calders et al. (2015) used a quantitative structure model modified from Raumonen et al. (2013) to directly infer tree volume as an estimate for AGB. They observed high agreement with destructive sampling (correlation coefficient of 0.98), and notably less agreement (0.68-0.78) for two allometric nondestructive techniques, DBH and tree height. Their TLS methodology was found to overestimate AGB by 9.68%, compared to Raumonen's relative error of ~2% and underestimation by the allometric equations of 30-37%. Yao et al. (2011) used TLS measurements of DBH, stem count density, and basal area to derive above-ground woody biomass at a plot level. They estimated AGB from the mean diameter and mean stem count based on allometric equations for the two dominant species and then compared the results to individual tree measurements, finding a strong 1:1 linear relationship (r^2 = 0.854). Site-wide, they found the r^2 increased to 0.975.

3.2.2.3 Shrubs. Shrublands have also been the subject of TLS studies. Olsoy et al. (2014a) compared TLS biomass estimates of sagebrush to destructive and point-intercept sampling. In total biomass prediction, TLS performed better than point intercept measurements (r^2 = 0.90 vs r^2 = 0.85). In green biomass (which they

distinguished by the intensity of the laser return pulses), TLS was much better than the point-intercept sampling employed (r^2 = 0.86 vs r^2 = 0.65). This research was expanded upon by Olsoy et al. (2014b) by comparing the convex hull method, which generates a convex polygon around the object to measure volume, to the voxel volume method used in Olsoy, et al. (2014a). The findings indicate that convex hull estimated total and green biomass more accurately (r^2 = 0.92 and 0.83) than the voxel method (r^2 = 0.86 and 0.73). This was attributed to occlusion of the interior structure of the shrubs, resulting in erroneous null voxels when utilizing the voxel method.

A similar comparison of methods was carried out by Greaves et al. (2015) in which they compared the voxel method to surface differencing for AGB estimates of arctic shrubs. In surface differencing, the maximum point height (i.e. max shrub height) was subtracted from ground points to generate vegetation height from which volume was calculated. They found the voxel method to be marginally better than surface differencing for close range plot data (r^2 = 0.94 vs 0.92), while surface differencing outperformed the voxel method in site wide variable range data (r^2 = 0.91 vs 0.82). In both of these studies, the authors concluded that the method used should be determined by the vegetation structure, with voxel volume preferable when full penetration of the vegetation can be assumed, surface differencing performing better when there are no irregular gaps in the canopy, and convex hull requiring a consistent biomass to volume ratio across the object.

Li et al. (2015) presented a similar comparison of volume models, adding a Triangular Irregular Network to the voxel volume and convex hull assessments. They also included a comparison of methods to delineate individual shrubs from TLS point

clouds via manual selection, segmentation, and neighborhood point statistics. The results were mixed, with voxel volume using manual delineation obtaining the highest adjusted r^2 (0.90), while the voxel volume with point statistic delineation having the lowest (0.51). In general, however, neighborhood point statistics did outperform segmentation despite slight underestimations of boundary, and the convex hull outperformed the voxel and TIN models, despite overestimations of volume.

3.2.3 TLS for Non-Woody Vegetation Assessment

3.2.3.1 Digital Elevation Models. One of the earliest applications of TLS was for the creation of digital elevation models (DEMs). Consequently, much of the research done with TLS in grass systems has focused on the challenges of obtaining proper ground measurements for the creation of DEMs rather than the direct measurement and assessment of grassland vegetation itself. Still, these studies provide valuable insight into the application of TLS in these systems.

Fan et al. (2014) demonstrated considerable occlusion laser returns from short grass (2.75-5.5 inches) on a mown lawn. Using a single scan location, they observed an average laser penetration depth of around 35% of grass height, which decreased with both grass height and distance from the scanner. Similarly, Nouwakpo et al. (2015) noted that due in particular to the use of a single scan location, error in TLS derived soil surface microtopography increased dramatically with vegetation cover.

Coveney and Fotheringham (2011) made a similar investigation on DEM error induced by dense ground vegetation in a flat coastal saltmarsh. This survey consisted of 11 scan locations scattered throughout the study site. Using gridded GPS data as validation, they found that the elevation error from vegetation occlusion and density was

significantly higher than all other survey or processing error sources combined. Using a ground-based elevation filter to select the lowest return in a 1x1m grid, they were able to reduce the elevation error by 40%. However, this method greatly reduced the resolution of the model. This supports the findings of Guarnieri et al. (2009), who used a combination of a moving window filter and classification of the return beam intensity to remove non-ground returns. While none of these studies attempt to derive biomass or vegetation structure from TLS data, obtaining an accurate DEMs as described here is a critical step in estimating above ground biomass.

3.2.3.2 Fuel Bed Modeling. The characterization of fine scale fuel bed components for fire prediction and modeling has been a strong stimulus in using TLS to characterize grasses. Of particular interest to many researchers has been deriving vegetation height, which is an important determinant in both fire modeling as well as AGB estimations. Loudermilk et al. (2009) measured understory fuel bed heights of forbs and prairie grasses in a second-growth longleaf pine forest. They found decent correlation between TLS derived height measurements and the point intercept method traditionally used (r^2=0.48, p=0.12). The discrepancies observed were explained by the overestimation of volume by traditional means due to variations in biomass distributions in shrub canopies. They concluded that TLS was preferable due to its lower nugget effect observed in empirical variograms and its sensitivity to small scale variation often missed with conventional estimations.

Rowell and Seielstad (2012) had similar findings with regards to the shortcomings of the point intercept method in describing fuel bed heights when compared to TLS. From TLS derived heights, they were able to accurately distinguish grass and litter from

shrubs, while forbs showed characteristics of both grass and shrubs. Interestingly, the highly similar pre-burn and post-burn bare earth measurements observed suggests that vegetation metrics (e.g., volume) can be developed from pre-burned vegetation height and post-burn ground measurements (Rowell and Seielstad 2012). In a bunchgrass dominated grassland, Umphries (2013) observed a similar relationship between TLS derived height metrics and field measurements. However, using only TLS derived bunch height, only ~30% of variation in the destructively sampled AGB was explained. The author suggested that including cover or volume metrics (e.g., Loudermilk et al. 2009 or Olsoy et al. 2014b) would better predict AGB than height alone. Wallace et al. (2016) were able to use multi-temporal TLS data to observe changes in a savanna understory fuel bed following a burn and through the system's recovery period. The authors were able to model changes in both fuel bed height and cover from TLS generated fuel bed maps that corresponded closely to conventional methods.

Schaefer and Lamb (2017) used a combination of the normalized difference vegetation index (NDVI) and TLS height metrics to estimate biomass in a Tall Fescue pasture, and found that using the two in conjunction produced better results ($r^2 = 0.76$) than using only TLS height ($r^2 = 0.61$) or NDVI ($r^2 = 0.56$) alone.

3.2.3.3 Agricultural Vegetation Assessment. The use of TLS for the characterization of non-woody vegetation has also been implemented in rangeland and agricultural studies. Radtke et al. (2010) implemented a downward facing TLS system to estimate the AGB loss from herbage removals that mimicked grazing patterns. They observed strong relationships between the change in TLS derived volume and measured dry weight AGB for the two rangeland species observed ($r^2 = 0.970$ for alfalfa and 0.57

for tall fescue). This high agreement was due in part to the low stature and homogenous sample plots, but the downward facing orientation of the scanner contributed significantly due to the reduction in occlusion often caused by the low scan angle of ground-based scanners. Andújar et al. (2013) used a similar downward facing TLS system to detect and discriminate between weed species in maize crops. Detection of the weeds was highly correlated to field measurements (r^2 = 0.88), but identification was only correct with 77.7% accuracy when *S. halepense* was compared against the other three as a group.

Hosoi and Omasa (2009) used their voxel based method to model vertical plant area density profiles of wheat. They were able to allometrically relate the dry weight of ears (r^2 = 0.96) and leaves and stems (r^2 = 0.94) with their TLS derived volumes. They additionally stressed the importance of the scanner's orientation, noting that the inclination used in this study (57.5°) allowed for both better penetration as well as helping with correction of leaf inclinations without leaf angle measurements. Eitel et al. (2014) used TLS derived volumes to estimate wheat biomass and nitrogen at different phenological stages of wheat, joining and tillering obtaining r^2 of 0.77 during tillering phases in 2011 and 2011, and r^2 of 0.79 in 2011 and 0.72 in 2012 for joining phases. This suggests some degree of uncertainty in the seasonality of measuring AGB

3.3 Structure-from-Motion for Vegetation Assessment

Structure-from-Motion (SfM) was first introduced as a computer vision technique by Ullman (1979), but it has only been with recent advances in computing that this method has been able to be applied efficiently. Similar to TLS, much of the early interest in SfM has been dedicated to topographical studies, particularly as a low-cost alternative

to TLS which requires much more specialized and expensive equipment. Little research has focused on applying SfM to vegetation assessment, however, and like the development of TLS, studies exploring SfM in vegetation analysis have largely focused on forested ecosystems, with limited application in assessment of fine scale vegetation such as grasses.

3.3.1 SfM Overview

Structure-from-Motion is a computer vision technique that generates a 3D point cloud similar to that of LiDAR. Unlike LiDAR, which is an active remote sensing system that generates the point cloud from direct measurements of an object, SfM is a passive method that generates a point cloud from a series of overlapping photographs. This process generates the 3D geometry of the target as well as the camera pose. This is accomplished through triangulation unique points identified on the target from matching points between at least three photographs of differing orientation (Figure 1, Thormählen et al. 2010). This generates the 3D location of the target points as well as the orientations and positions of the cameras.

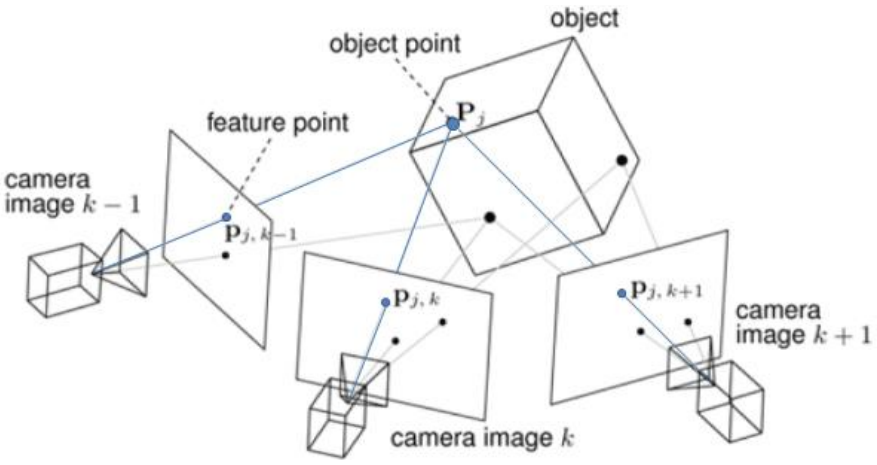

Figure 1. Conceptual visualization of SfM (from Thormählen et al. 2010).

Specialized software (e.g., Agisoft Photoscan, as used in this study) finds common points automatically in overlapping photographs to generate a 'sparse point cloud' and to calculate the position and attitude of each photograph. Then a more detailed point cloud is generated, often with a point density comparable to or greater than TLS systems and with red, green, blue radiance values from the best fit digital photograph pixel corresponding to the 3D point. Placement of distinct targets around the object aids the SfM matching process, and can be used subsequently to help georeference the point cloud, which is generated without any spatially explicit reference system. This new point cloud can be manipulated directly much like TLS derived point clouds, and with proper georeferenceing datasets may even be combined. A polygonal mesh representative of the target's surface can also be generated and used for a variety of analytical purposes such as DEM generation and volumetric measurements.

3.3.2 Comparisons between SfM and TLS

SfM offers both advantages and disadvantages over TLS techniques. It has been noted that data acquisition can be much quicker for SfM than for TLS scans (Nouwakpo et al. 2015), though TLS scan time varies greatly based on the unit specifications. Furthermore, the relatively low cost and high portability of equipment makes this a much more accessible technology than TLS. These advantages are traded off for specialized software needed and added processing time to generate the point clouds (Nouwakpo et al. 2015; Morgenroth and Gomez 2014).

Like TLS, SfM measurements can be obtained out without any prior referencing or calibration, as SfM point clouds are generated only from the input photographs. SfM point clouds are generated without any reference unit. Rather, the relative distance of

points to one another is arbitrary and must be established by identifying reference objects with known locations to scale to point cloud to. TLS conversely generates point clouds in reference to the scan location and are generated with a meaningful relative scale (in meters) that can be measured directly. This means that SfM point clouds must be manually georeferenced adding to SfM's already increased processing time.

Early implementation of SfM, like TLS, has focused on topographical studies, though from these studies possible applications to vegetation assessment can be seen. Nouwakpo et al. (2015) used SfM and TLS to derive soil microtopography in plots with varying degrees of vegetation, and made several observations on the utility of SfM and TLS. They observed that with increasing vegetation cover, the agreement between TLS and SfM degraded slightly, with significant divergence beyond 53% ground cover. They attributed this to the difficulty of the SfM software (Agisoft PhotoScan) in correctly matching vegetation pixels due to similarities in heavily vegetated areas. Furthermore, the surfacing of the SfM point cloud tended to smooth out irregularities, resulting in a narrower range and loss of fine scale detail. For grasses in particular, they observed that increasing grass cover lead to an increase in signal to noise ratio in both TLS and SfM. Two different configurations for SfM analysis were used in their study. The first two years of the study, photos were taken from a frame directly above the plots, yielding near nadir views. The third year photos were taken by hand around the perimeter of the plot. They observed that the increased obliquity allowed for more accurate measurements around the vegetation resulting in more accurate elevation models.

Liang et al. (2014) compared SfM to terrestrial LIDAR measurements in a mature mixed forest during winter months. They estimated DBH of trees in a 30 x 30 m plot,

taking photos approximately 20 cm apart around the plot perimeter. Both SfM and TLS had an overall stem mapping accuracy of 88%, however SfM DBH measurements yielded slightly better results (RMSE of 6.60% vs 7.27% for TLS). While SfM has been applied much more sparsely to vegetation assessment than TLS, these results clearly show SfM is capable of producing results of comparable accuracy to those of TLS.

3.3.3 SfM for Woody Vegetation Assessment

The use of SfM in vegetation assessment has primarily focused on linear measurements such as tree height or diameter at breast height (DBH). Hesse (2014) used SfM to map vegetation cover and height in sand dunes. He used a camera mounted approximately 6m above the ground, and noting the importance of obliquity to the measurements, the camera was angled 30° from nadir. He found SfM plant height to be largely in agreement with field measurements, however he noted that the depth filtering employed sometimes removed the top portions of the vegetation, a trend that could prove problematic for volumetric measurements with SfM.

Morgenroth and Gomez (2014) used SfM in conjunction with Multiple View Stereophotogrammetry to measure individual tree height and stem diameter for a young deciduous, a mature deciduous, and a mature pine tree. Their results were very accurate, with height error of 2.59% and stem diameter error of 3.7%. While shadowing was found to be problematic in correctly registering points, they observed that distance from the camera appeared to have no linkage to error. This is in contrast to previous findings (James and Robson 2012) which established a relationship between accuracy estimates and distance to the photopoint as a ratio of approximately 1:1000.

In making DBH estimations of trees in a 30 x 30 m, Liang et al. (2014) found that most of the error from SfM measurements occurred in the central portions of the plot and were the result of occlusion, shading, and increased distance from the camera. In 2015, the authors added to their 2014 findings, using an internal path taking photos outward from within the plot in addition to the perimeter photos facing inwards (Liang et al. 2015). They found RMSE for DBH to be between 8.03 and 18.87% depending on the paths and camera orientations used. The best configuration was found to be from the outer path using a landscape camera configuration, which generated more accurate point clouds than those generated using a portrait view or outward facing photographs. These results compared relatively well to the 9.74% RMSE for TLS derived DBH. Liang et al. (2015) also reported significant influence of distance on their measurements, with further observations containing lower point densities and more noise. The distance induced error observed in both Liang et al. 2014 and Liang et al. 2015 was in contrast to Morgenroth and Gomez's 2014 findings that distance didn't contribute to error. This could be explained by the different scales, with Morgenroth and Gomez taking photos directly around the tree of interest, while Liang et al. in 2014 and 2015 assessed individual trees from photographs of a 30x30 meter plot.

Miller et al. (2015) was the only study found that used SfM to directly obtain volumetric estimates of vegetation. They measured the height, diameter and volume of 30 leafless deciduous trees. Photo acquisition consisted of 2-3 rows of photos around each tree (resulting in 150-180 photos per tree) and found the volumetric measurements of the main stem to be highly accurate and consistent with destructive measurements (RMSE 12.33%, r^2 = 0.968). Smaller branches were much more difficult to model, with

RMSE of 47.53% and r^2 of 0.761. Overall, however, the RMSE was 18.53% while the r^2 was 0.951. Furthermore, a consistent bias to underestimate tree volume was observed, particularly with smaller branches at the extremities. They also noted the influence of ambient light on the measurements, recommending a diffuse rather than direct light source if possible in order to minimize over exposure and high contrast images, as well as taking measurements in as short a time frame as possible (ideally around noon with minimal shadows) to avoid inconsistencies in lighting. These observations highlight the possible difficulties of obtaining SfM derived measurements of fine scale vegetation, particularly open grassland environments.

3.3.4 SfM for Non-Woody Vegetation Assessment

The only study found that focused on fine scale vegetation (i.e. grasses) using ground based SfM was Nouwakpo et al. (2015). This study, however, simply looked to quantify the occlusion that resulted from ground vegetation occluding the soil surface when generating a DEM. While SfM has yet to be applied to assess grassland vegetation directly, the technology is promising and studies show consistent agreement between SfM and TLS measurements. However, using SfM to obtain volumetric estimates of fine scale vegetation has been shown to be difficult, particularly with regards to obtaining reliable ground points and movement of vegetation between scans or photos.

4.0 MATERIALS AND METHODS

4.1 Study Site

Field measurements were collected in September and October 2016 on the North Farm Unit of Oak Lake Field Station in Eastern South Dakota when adequate wind conditions were met. The field station has been affiliated with South Dakota State University since 1988, and the North Farm Unit has not been subject to any form of management practice (e.g., grazing, burning, haying, etc.) since that time. Consequently the unit is dominated by Smooth Brome grasses (*Bromus inermis*), an invasive cool season grass. The North Farm Unit at OLFS was chosen primarily for the homogeneity of grass species present. This homogeneity was due in large part to the absence of any disturbance regime, either natural or anthropogenic. However as a result of this, a large undisturbed littler layer was present throughout the site.

The field station is located on the Northern Glaciated Plains and has a mid-continental climate. Peak precipitation occurs in July, with mean annual precipitation of 58 cm and a mean annual temperature of 6.1°C from 1995 to 2015 (SDSU Mesonet). All plots were located on upland sites with well drained, fine-loamy soils in the Singsass-Buse soil complex (Soil Survey Staff). Sites were selected in flat areas, and all sites were relatively flat, with slopes of less than 5°.

Data collection was limited to windless days or on days with low wind (<5 mph) for plots in wind shadows (due to nearby woodlands). The measurements were made under consistent solar conditions (either overcast or clear skies) to avoid any variation in lighting conditions during the photo capture that might lead to poor photographic alignment (Miller et al. 2015).

Within the North Farm unit, eleven 1 x 1 m plots were delineated by four 1.2 m tall poles. The poles were 0.8 cm in diameter, and had a 25 cm white reflective band that produced notably higher TLS return intensities than the surrounding vegetation. The height of each reflective band above the surface of the ground was measured at each site and were used in point cloud alignment and in determining ground points. Additionally, painted 7.6 cm cubed targets were placed on top of each pole to aid with SfM photographic alignment (Figure 2).

Figure 2. Destructive sampling of aboveground grass biomass in one of the grassland plots. The four poles roughly delineate the 1 x 1 m plot and were used as reference points for aligning the SfM and TLS point clouds.

Plots were selected across a range of grass heights observed at the field station, with average heights ranging from approximately 50 to 70 cm. As data collection occurred late in the growing season, the grasses had reached full maturity and a minority of seed heads were present in all plots and had heights ranging from 90 to 120 cm. Non-

grass vegetation was excluded in plots selection and the homogeneity of grass species present was maximized.

4.2 Data Collection

4.2.1 Hardware

TLS data was collected using a Compact Biomass Lidar (CBL) (Kelbe et al. 2013; Paynter et al. 2016). The CBL is optimized for rapid scanning and portability. It uses a SICK LMS151 LiDAR unit that records time of flight and intensities of first and last returns with 360° horizontal and 270° vertical views in approximately 33 seconds. The unit has a 0.25° angular resolution, a beam wavelength of 605 nm, and a 0.86° beam divergence and a maximum range of 40 m.

Photographs for SfM point cloud generation were collected using a Canon EOS 6D 20 Megapixel digital single-lens reflex camera. A Canon EF 24-70mm f/4L IS USM lens was used that is stabilized and has low dispersion aspherical detector elements to minimize chromatic and spherical aberration and color blurring around subject edges. The lens coatings provide improved color rendering and minimal ghosting compared to standard lenses and are resistant to dust and water. During photo capture a constant focal length of 24 mm was used.

SfM photographic alignment was done on a Dell PowerEdge R815 linux server operating with a 4 socket, 48c AMD Opteron™ Processor 6348 at 2.8 Ghz and 512 GB DDR Ram.

The disc pasture meter used in this study was constructed in the manner of Rayburn (1997; Rayburn and Rayburn 1998), and consisted of a 0.4572 x 0.4572 m (18 x

18 inch) weighted acrylic plate. A meter stick measured from a large central hole is used to record the disc pasture meter's settling height once it has come to rest on top of the grass.

4.2.2 Remotely sensed data collection

4.2.2.1 TLS. A total of four TLS scans were taken from opposing sides of each plot to minimize occlusion effects on vegetation assessment (Van der Zande, 2006). The CBL unit was mounted on top of a tripod, and a spirit level was used to ensure the CBL was level throughout each scan. The resulting point clouds were therefore properly oriented to two horizontal dimensions (x, y) and one vertical dimension (z). The CBL sensor height was 1.6 m above the ground which ensured that the CBL was always above the grass (heights 50 to 70 cm). Due to a structurally induced occlusion area of 45° off nadir, TLS scans were taken 1.6 m away from the plot edge, which corresponded to the scanner height. Remotely sensed grass was therefore between 1.84 m and 2.80 m away from the CBL. At these ranges the LiDAR pulses were sensed every 0.80 to 1.22 cm (due to the 0.25° angular resolution) and given the 0.86° beam divergence each pulse width is 2.76 cm to 4.2 cm. As the grass blades were typically less than a millimeter thin and less than 1 cm across with any orientation many of the LiDAR measurements were partial returns.

4.2.2.2 SfM. Approximately 150 overlapping photographs were taken in concentric circles approximately 1.5 m from the center of each plot. Photos were taken by hand approximately 20 cm apart by taking a small step clockwise around the plot after each photo. Several passes were made at varying heights so that full hemispherical coverage of the plot and adequate photographic overlap (greater than 60%) was obtained.

The camera parameters were manually selected based on ambient light conditions during photo acquisition. Specifically, a minimal ISO was a priority to provide finer grain digital photographs. Aperture was kept small to maximize the field of view and an adequate shutter speed was used so that sharp images of the plots with low noise were captured. Photo capture took approximately 10 minutes per plot.

4.2.3 Disc pasture meter

After TLS and SfM data collection, one end of a meter stick was carefully placed on the ground surface at the center of the plot. The meter stick was placed through the central whole of the disc pasture meter, and the disc pasture meter was then gently lowered on top of the grass taking care to ensure the disc did not contact the meter stick. The settling height of the disc was recorded to the nearest millimeter at the center of the disc.

4.2.4 Destructive sampling

A wooden frame that encompassed the disc pasture meter was placed around the disc pasture meter at the center of the plot and the grasses were parted so that the frame rested on the ground. All vegetation within the frame was clipped to ground level (Figure 2). In each plot there was a non-negligible litter layer on top of the soil surface. As neither TLS nor the digital photographs for SfM point cloud generation were able to penetrate the grass canopy and resolve the litter layer, it was removed from the standing vegetation and bagged separately.

All grass and litter samples were dried at 60°C for 72 hours and then independently weighed with an accurate laboratory scale and converted to AGB in units g/m^2 by dividing the measured weight by the 0.4572 x 0.4572 m area from which the

grass was harvested. Weights were tabulated as total dry weight AGB (AGB_{total} = litter dry weight + standing vegetation dry weight) and grass dry weight AGB with litter removed (AGB_{grass} = standing vegetation dry weight only).

After vegetation had been removed from the plot and bagged, TLS and photographic data were collected again using the same methodology in order to obtain an observed ground surface without vegetation occlusion. The height above the ground surface of the white reflective band on each corner pole was measured and recorded so that an estimated ground surface could later be generated for comparison to the observed ground surface.

4.3 Point Cloud Generation and Alignment

The general workflow of data processing to generate volume estimates is outlined in Figure 3. Three dimensional point clouds composed of x, y, z coordinates relative to the scanner location were generated onboard the CBL unit. SfM point clouds were generated from the digital photographs using Agisoft Photoscan Pro 1.2.4 (Agisoft LLC, 2016) and processed on a high performance Linux server.

SfM point cloud generation was completed in three stages. First, where necessary shadows cast by the photographer were manually masked from the photographs using Photoscan in order to avoid inconsistent lighting and to allow for accurate point identification. Next, the masked images were aligned from unique points automatically identified in overlapping photographs by Photoscan. During this process, Photoscan calculated the camera position and attitude, and a sparse point cloud defined by the identified unique points was generated. From this, Photoscan generated depth maps for

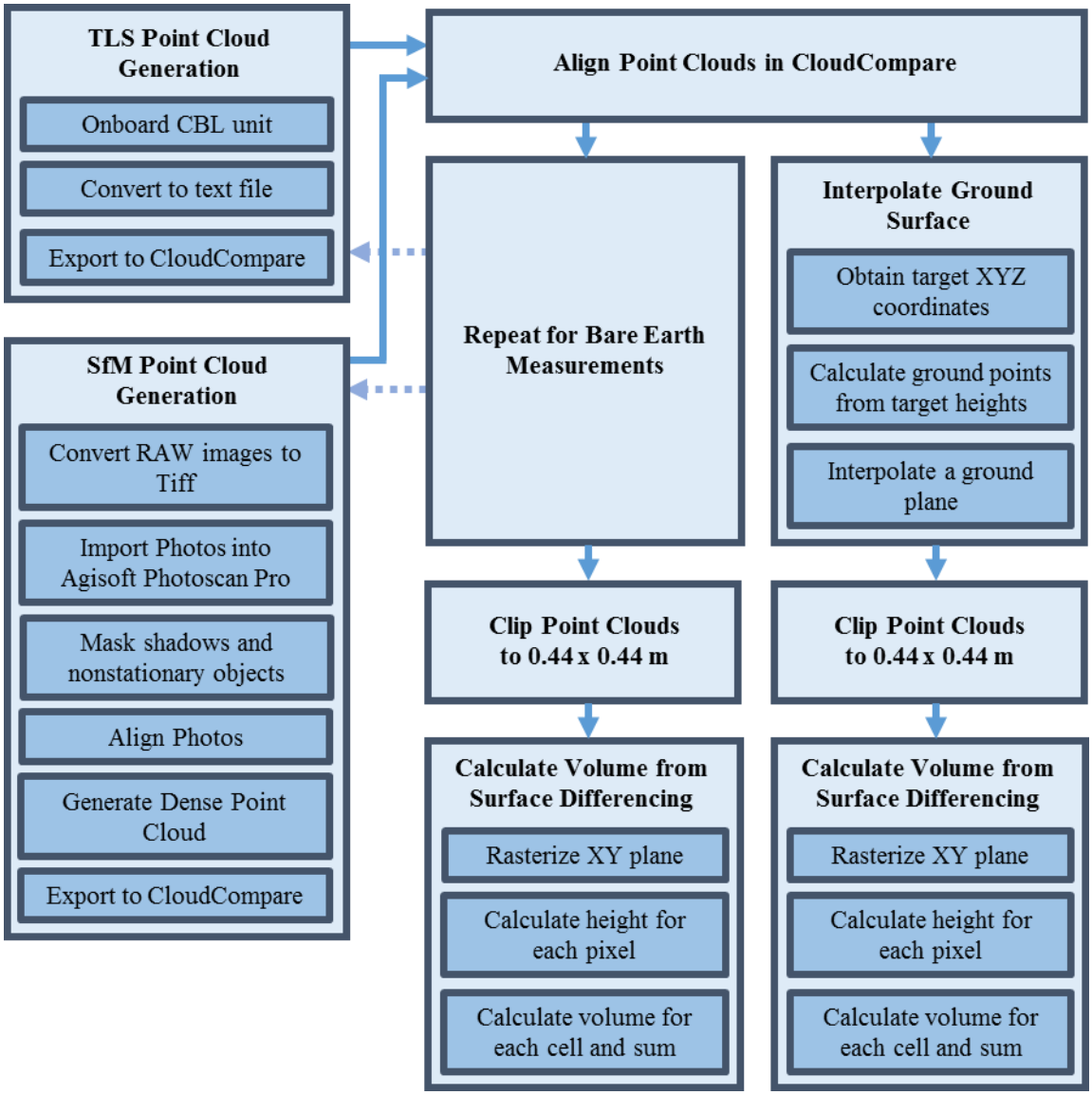

Figure 3. Processing workflow of TLS and SfM volume estimation. SfM point clouds were aligned to TLS point clouds, but save for that the two processes remained entirely separate. The result was two volume estimates per plot for both TLS and SfM point clouds, one derived from the observed bare earth measurements, and one derived from the estimated ground surface.

each photo, from which a dense point cloud was generated with point densities many times greater than the sparse point cloud.

Due to the highly homogenous appearance of the grass, feature matching of the grass plots during the photo alignment phase was difficult. Using high accuracy settings

resulted in poor model outputs and large gaps in the point cloud, therefore a low accuracy setting was used. This also greatly reduced processing time required for photo alignment. Within the software, a depth filtering parameter was used to automatically remove erroneous points from the dense point cloud. A mild depth filtering setting was found to produce the most reliable dense clouds, as aggressive depth filtering led to an over-smoothing of the vegetation surface and removed the upper portions of the vegetation, while disabling this feature resulted in excessive noise rendering the point cloud unusable.

SfM point clouds are generated without any meaningful spatial scale or reference and must be manually georeferenced to apply a meaningful scale for analysis. SfM point clouds were therefore aligned to the appropriate TLS point cloud to take advantage to the spatially explicit nature of TLS point clouds.

All point cloud alignment and analysis was carried out using CloudCompare 2.7.0 (CloudCompare, 2017). For each of the eleven plots, the four TLS point clouds were aligned and combined using CloudCompare to manually select equivalent point pairs and generate an appropriate transformation for the entire point cloud. In each scan, the reflective bands on all four poles were readily apparent, and the bottom of each band was identified in each point cloud to generate the point cloud transformations.

SfM point clouds were aligned to the equivalent TLS point cloud using the same methodology as well as the painted pole top cubes. This process was repeated for the observed ground surface TLS and SfM point clouds that were collected after biomass removal. The observed ground surface was used to identify the harvested area, and all point clouds were clipped to a 0.44 x 0.44 m square within that area.

4.4 Volumetric Assessment

Various methods have been proposed to estimate AGB from 3D point clouds. While some methods use point cloud measurements to estimate AGB from other allometric relationships (e.g., TLS derived DBH to estimate tree biomass (Morgenroth and Gomez 2014), of particular interest to this study is the use of volume estimation to derive AGB. Several methods have been proposed that use point cloud derived volume estimates to estimate AGB, and each requires different assumptions of vegetation structure to accurately relate volume to AGB.

Sophisticated methods have been proposed to estimate vegetation AGB from 3D point clouds using quantitative 3D vegetation models to generate complex and highly accurate volumetric models (Raumonen et al. 2013). However, these approaches are inappropriate for application to grasses unless the individual grass components can be resolved in the point cloud which was not the case for this study.

The voxel volume method (Hosoi et al. 2006) divides the three dimensional space occupied by the point cloud into 3D pixels, or 'voxels', of a specified size. Whenever a point is observed within one of these voxels, that voxel is classified as vegetation. By summing the volumes of all the vegetation voxels, one can obtain the overall volume of a target. Any occluded region of the target would not be classified as vegetation regardless of vegetation presence or absence. This process therefore assumes full penetration of the vegetation, as any occluded regions would result in erroneously low volume estimates.

The convex hull method (Olsoy et al. 2014) generates a 3D convex hull bounded by a set of outer points such that the entire point cloud is located within the convex hull. Volume can then be calculated from the interior of this object. In relating this method to

AGB it assumes equal distribution of vegetation density across the vegetated area. Neither TLS nor SfM can fully penetrate grass canopies (Fan et al. 2014; Nouwakpo et al. 2015), and grass density varies by height, particularly in mature stands such as those being studied. This study therefore employed a surface differencing method (Greaves et al. 2015; Eitel et al. 2014) for volumetric measurements, which calculates vegetation volume from the area between a vegetated surface and a ground surface (Figures 4 - 7). As neither TLS nor SfM point clouds have any reference to the ground surface, an estimated ground surface first needed to be defined in order to estimate the grass volume.

Although the plots were on flat (< 5°) sites, a planar model of the ground surface was defined. The x, y, z coordinates of the bottoms of the white reflective bands on each pole were identified in the aligned 3D point clouds. Then the measured distances from the bottoms of the white reflective bands to the ground surface (Section 4.1) were subtracted from each z coordinate. This yielded four x, y, z coordinates defining the location of the ground at the base of each pole relative to the point clouds. The ground surface was defined by two 3D triangles with vertices defined by the pole coordinates.

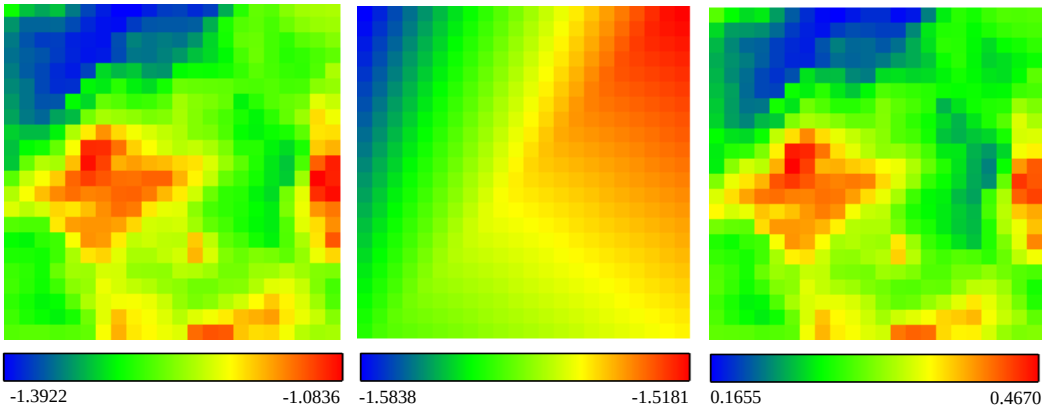

Figure 4. Visualization of surface differencing method employed (shown: 2 x 2 cm cells). The mean z-coordinate value (m) for each 2 x 2 cm estimated ground surface cell (center) was subtracted from mean SfM z coordinate value for the vegetation cell (left) to yield the relative height of grasses in each cell (right).

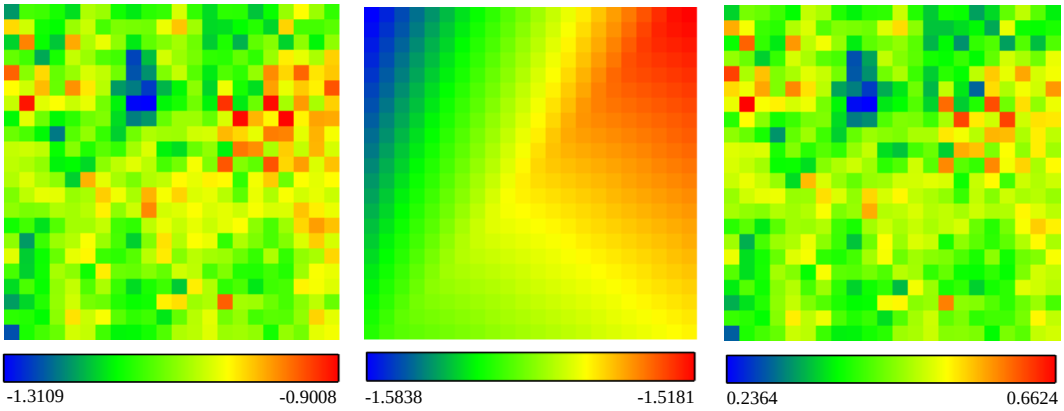

Figure 5. As Figure 4 but using the TLS derived vegetation heights (left) and the estimated ground surface (center) to generate the relative grass heights (right) rather than SfM vegetation heights.

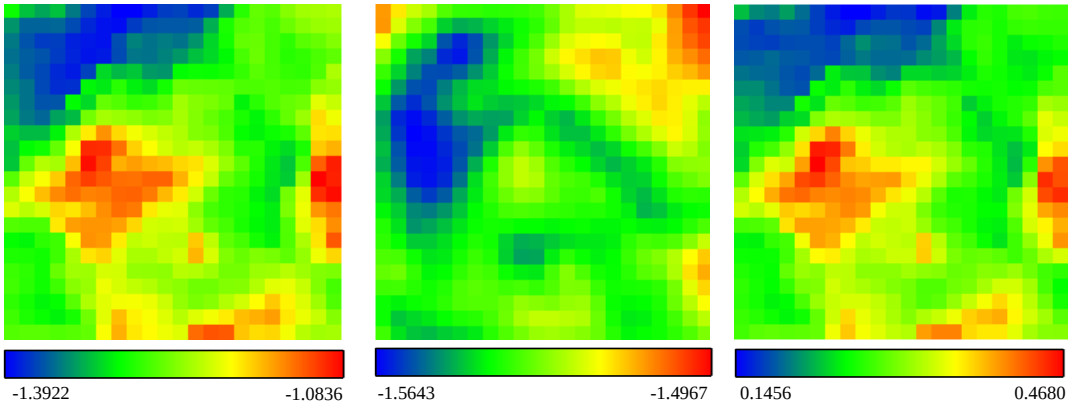

Figure 6. As Figure 4 but using the SfM observed ground surface (center) to generate the relative grass heights (right) rather than the estimated ground surface.

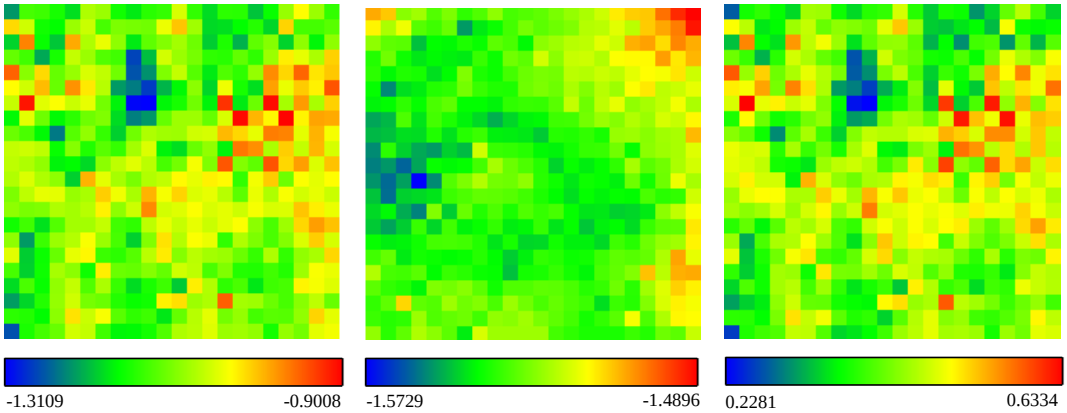

Figure 7. As Figure 5 but using the TLS derived observed ground surface (center) to generate the relative grass heights (right) rather than estimated ground surface.

Volumetric measurements were carried out using CloudCompare's 'Compute 2.5D volume' function using both the estimated ground surface (Figure 4 and 5) and the observed ground surface (Figure 6 and 7). This process relies on rasterizing the x,y plane into square cells of a specified width. For each cell, the mean relative height of grass above ground level was calculated as:

$$\text{mean relative height} = \frac{\sum z_{canopy\ points}}{n_{canopy\ points}} - \frac{\sum z_{surface\ points}}{n_{surface\ points}} \quad (1)$$

where $z_{canopy\ points}$ and $z_{surface\ points}$ are the vertical values (z coordinates) of TLS or SfM points falling within the x,y dimensions defined by the cell, and n is the total number of points within each cell. The resulting relative height metric is equivalent to the mean height of grass above ground level within each cell. From this, the grass volume of each cell was derived by multiplying the cell side dimensions and the cell's mean relative grass height. Total plot volume was calculated by summing the volumes of all cells within the plot.

The volume derived by the above process is expected to be sensitive to the cell dimension in a complex way relative to the structure of the vegetation and the resolution provided by the TLS and SfM measurements (Greaves et al. 2015; Eitel et al. 2014). To assess this sensitivity, AGB estimations were made using volumes calculated from cell dimensions with widths of 0.5, 1, 2, 4, 11, 22, and 44 cm were considered. Note that the 44 cm cell dimension is equivalent to simply using the mean plot vegetation height, which is similar to previous grass AGB research approaches (Umphries 2013; Schaefer and Lamb 2016).

4.5 Allometric AGB Estimation

Statistical analysis and generation of allometric regressions were carried out in R (R Core Team 2015). The volume estimates derived from TLS and SfM point clouds as well as the settling height of the disc pasture meter were linearly related to the destructively sampled AGB of the grass plot through ordinary least squares regression (OLS) both with (AGB_{total}) and without litter (AGB_{grass}) included in the regression. The performances of the resulting models were then evaluated using the coefficient of determination (r^2) as well as the F-test p-value.

The OLS regression terms for the settling heights have different units (cm) to the point cloud grass volumes (m^3) and so they cannot be compared directly. Therefore to compare the predictive capability between the three models a boot-strapped "leave one out" cross validation (LOOCV) approach was adopted in which the regressions were repeatedly generated each time leaving out one observation for model validation and using the remaining ten as training data to generate the regression. From these regressions the following terms were defined:

$$residual_i = AGB_i - \widehat{AGB} \quad (2)$$

$$RMSE_{LOOCV} = \sqrt{\frac{\sum_{i=1}^{11} residual_i^{\,2}}{11}} \quad (3)$$

where $residual_i$ is the difference between the sampled AGB for 'left out' plot *i* (AGB_i) and the predicted AGB derived using the OLS regression derived using the data for the 10 other plots ($\widehat{AGB}$). The $residual_i$ was calculated for each of the 11 LOOCV runs, as were the OLS regression goodness of fit (r^2), F-test p-value, and RMSE. The $RMSE_{LOOCV}$ *i*s the root mean square error of the residuals of each of these regressions. This LOOCV methodology was implemented for each combination of

method (TLS, SfM, and disc pasture meter) and AGB (AGB_{total} and AGB_{grass}) investigated.

To investigate the relationships between total AGB and grass AGB with the litter layer removed, a reduced major axis (RMA) regression performed between the respective variables. An RMA regression was deemed more appropriate than OLS for this analysis because errors in the x and y axes for these regressions are likely to both be present in similar magnitudes, and the asymmetry between variables in OLS would be inappropriate for this assessment (Smith 2009). An RMA regression was also used to investigate the relationship between SfM and TLS volumetric measurements.

5.0 RESULTS

5.1 Destructive AGB Measurements

The destructively sampled grass and litter AGB (AGB_{total}) varied from 149 g/m^2 to 1043 g/m^2 (mean = 634.03 g/m^2). This range of AGB is comparable to those found in other undisturbed grass systems (Briggs and Knapp 1995) and managed smooth brome pastures (Lamond et al. 1992). The litter was highly variable, and ranged from 49.13 g/m^2 to 590.87 g/m^2, accounting for 13 - 57% of AGB_{total} at each site, with an average of litter proportion of 36% of AGB_{total} (Figure 8).

Because neither TLS nor SfM were able to penetrate the grass canopy and resolve the litter layer, AGB_{grass} was tabulated by removing the litter layer in order to assess its impact on AGB estimation (section 4.2.4). AGB with the litter layer removed reduced the range of dry weight AGB_{grass} to between 99.5 g/m^2 and 551 g/m^2 (mean 382.7 g/m^2). This nearly halved the range of observed values from a difference of 894 g/m^2 with AGB_{total} to 451 g/m^2 for AGB_{grass}. It was observed that sites with higher AGB_{total} tended to have a larger proportion of litter, as seen by the divergence from the 1:1 line in Figure 8. The high litter biomass was likely because the study site was not mown or grazed by domestic animals, or subject to prescribed fires, for at least two decades. High levels of litter accumulation in undisturbed grass systems such as this are not uncommon, and have been observed to be as high as three times the AGB of living vegetation (Weaver and Rowland 1952).

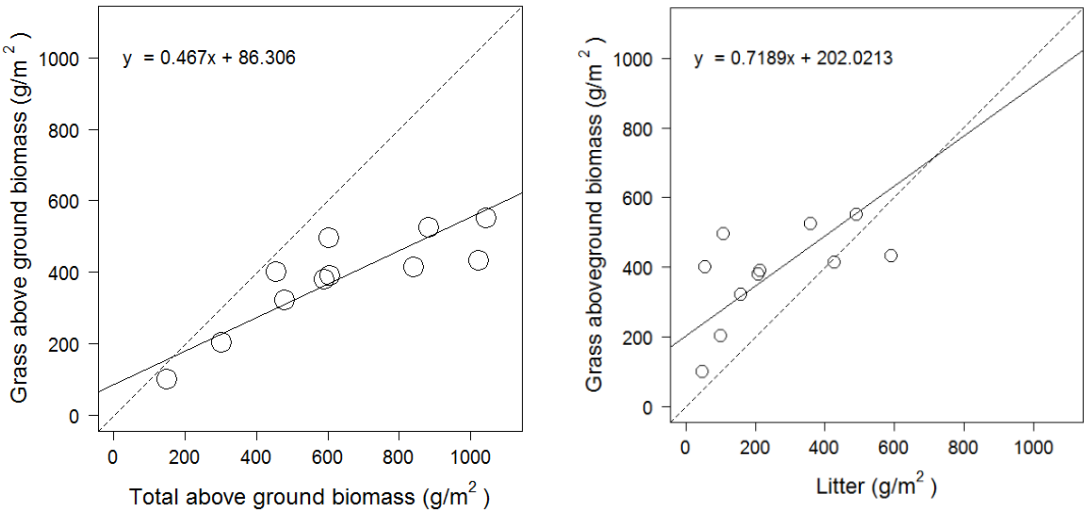

Figure 8. Destructively sampled AGB for the 11 plots. The AGB_{grass} and the AGB_{total} (left) have a 0.85 correlation, and the AGB_{grass} and litter AGB (right) have a 0.59 correlation. The solid line shows the reduced major axis (RMA) regression of these data and the dotted line shows the 1:1 line for reference.

5.2 Point Cloud Volumes

SfM and TLS were observed to generate morphologically similar point clouds but with significant differences in detail of the same grassland plot. A visual assessment of the generated point clouds confirms these differences. For reference, Figure 9 shows the same example point clouds of a typical plot (AGB_{total} = 602.7 g/m^2) as displayed in Figures 4 - 7. For all plots, neither TLS nor SfM provided canopy penetration to the ground or litter layers. Point cloud densities vary considerably, with TLS point clouds containing an average of approximately 4,000 points per 0.44 x 0.44 m plot, and SfM containing an average of nearly 35,000 points per plot.

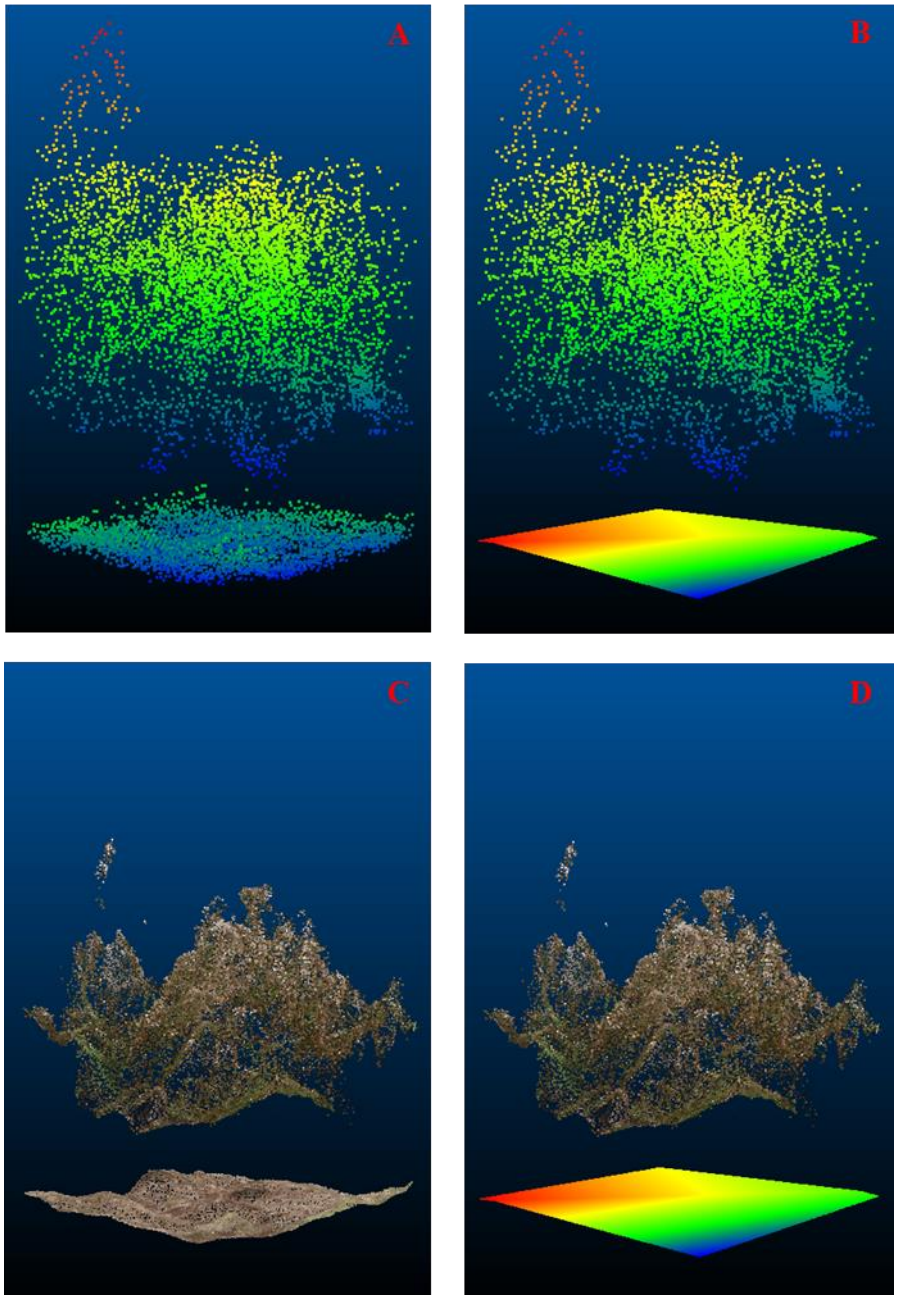

Figure 9. TLS (A & B) and SfM (C & D) top of vegetation point clouds used in the analysis for a typical grassland plot. The observed ground surface SfM and TLS point clouds collected after biomass removal are shown below the vegetation canopies (A & C), as are the estimated ground surfaces (B & D). The two SfM point clouds (C & D) are colored with the best fit digital photo red, green, blue radiance pixel value. The TLS point clouds (A & B) are colored by their relative height, as are the estimated ground surfaces (B & D, lower).

While point clouds generated from SfM display a readily identifiable vegetation canopy with structural detail, TLS generated clouds that were highly noisy and distinguishing a clear vegetation surface is difficult. This resulted from some of the isolated elements at the top of the canopy (i.e. taller grass blades and seed heads) present in all plots being expressed in TLS and SfM point clouds differently. TLS point clouds generated a significant amount of noise around seed heads (Figure 9a) due to partial hits and slight alignment errors between scans. Conversely, SfM failed to model the full extent of the seed heads (Figure 9b) due to SfM depth filtering. Though this was minimized, disabling depth filtering during SfM point cloud generation resulted in a high number of noisy mismatched points that rendered the point cloud unusable. This failure of SfM to model the full extent of grass height is evident across the plots, as is the high level of noise in TLS point clouds.

Volumes derived from TLS and SfM point clouds showed very little sensitivity to variation in cell sizes above 2 x 2 cm (Figure 10). However, at 1 x 1 cm and 0.5 x 0.5 cm cell sizes, volume metrics were markedly lower than for all other cell sizes. This resulted from empty cells within the plot dramatically lowering calculated volume as the cell size became smaller than the point cloud density, and thus being potentially calculated as not containing any vegetation volume despite the presence of vegetation. This trend was less pronounced in SfM volume estimations due to the higher point density of SfM compared to TLS.

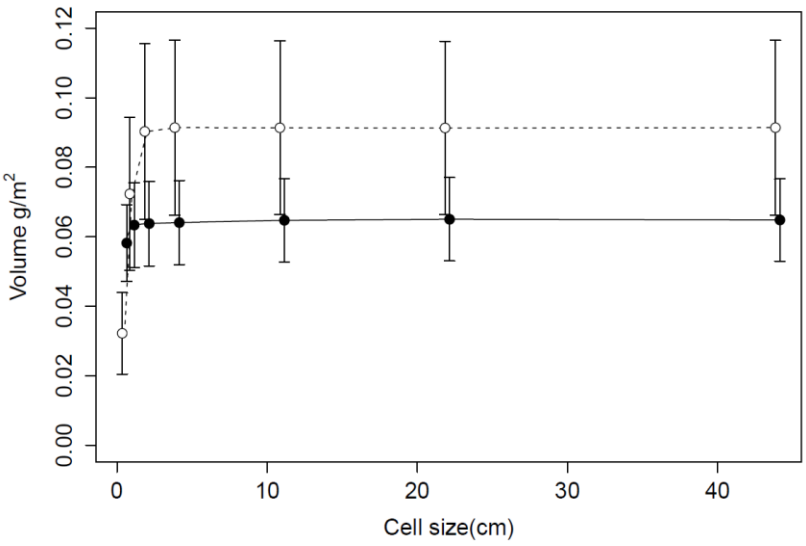

Figure 10. Sensitivity cell size of volumetric measurements using the estimated ground surface. Mean and standard deviation of TLS (open circles) and SfM (closed circles) volumetric measurements using the estimated ground surface. Cell sizes displayed had 0.5, 1, 2, 4, 11, 22, and 44 cm sides. Note that the 44 cm cell dimension is equivalent to simply using the mean plot vegetation height for this assessment.

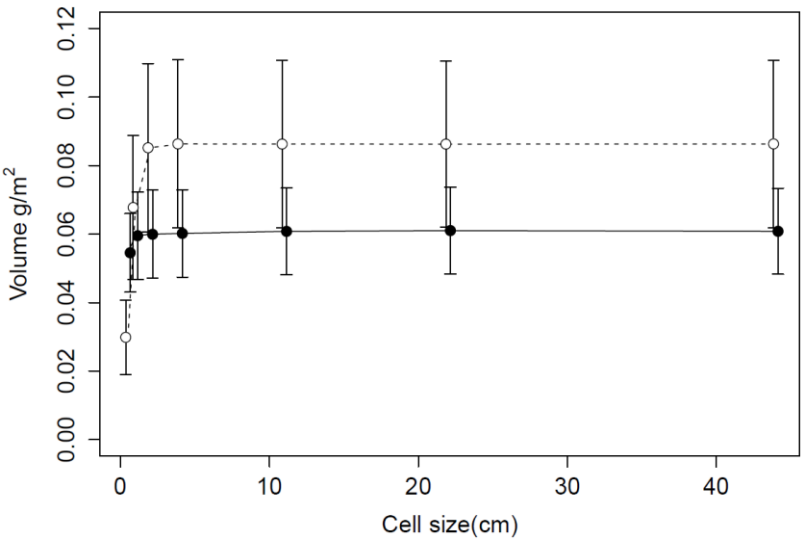

Figure 11. As Figure 10 but using the observed ground surface rather than the estimated ground surface for volumetric measurements

Sensitivity in volume estimations using the observed ground surface showed similar characteristics to those derived from the observed ground surface (Figure 11). Volume estimation was lower for both TLS and SfM when using the estimated ground surface, but the same insensitivity to cell size observed was observed.

With cell dimensions of 2 × 2 cm there were always points within each cell for the TLS or SfM point clouds. Because both TLS and SfM showed very stable volume estimates above this size, the remainder of the analyses were carried out using point cloud volumes derived with 2 cm cell dimensions. Further work is needed to establish the maximum optimal cell size for volumetric analysis of an undisturbed grassland plot.

A comparison of TLS and SfM volumes confirms differences observed between TLS and SfM point clouds. SfM derived grass volumes have a smaller range and are typically 27% less than the TLS derived volumes. This can be clearly seen the reduced major axis (RMA) regression of TLS and SfM derived volume estimates (Figure 12), which shows a significant divergence from the 1:1 line. Despite this bias, TLS and SfM volume estimates using the estimated ground surface are well correlated ($r = 0.762$), confirming that both methods are providing related measurements. This relationship was slightly weaker with volume estimates derived from the observed bare earth surfaces ($r = 0.738$), which showed a larger range in both TLS and SfM volume estimates thanks to topographical variation within the plot not captured by the estimated ground surface.

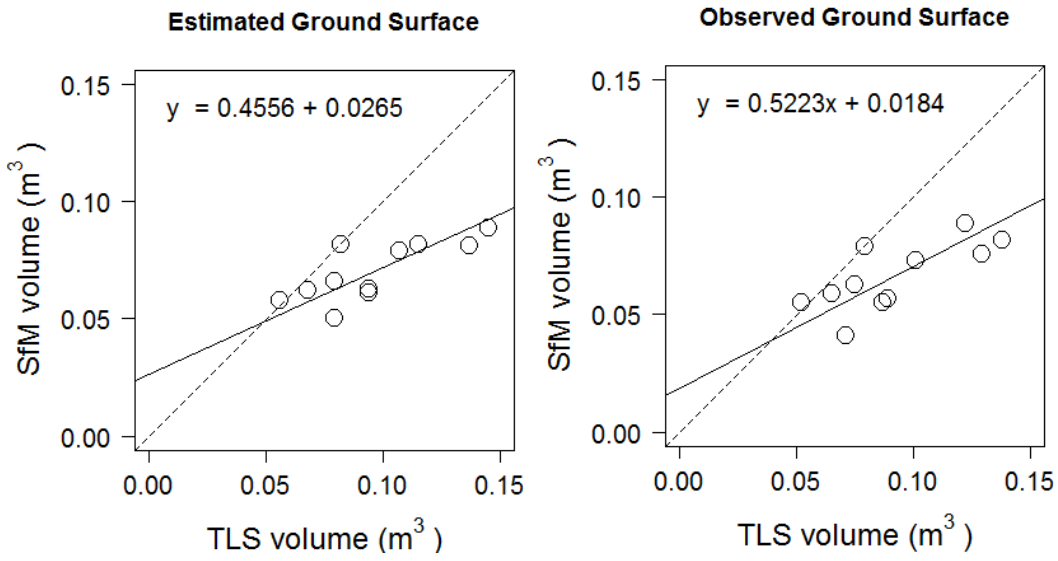

Figure 12. TLS and SfM volume estimates (m^3) derived from the 11 grassland point cloud data sets using the estimated ground surface (left, correlation 0.762) and the observed ground surface (right, correlation 0.738) and a 2x2 cm cell size. The solid line shows the reduced major axis (RMA) regression of these data and the dotted line shows the 1:1 line for reference.

5.3 AGB Estimation

The destructively sampled above ground biomass with (AGB_{total}) and without litter (AGB_{grass}) were compared by OLS regression with the disc pasture meter settling heights and with the grass volumes derived from TLS and SfM point clouds.

The disc pasture meter settling height was found to have the poorest regression fit with the destructively sampled AGB (Figure 13). Using the disc pasture meter, better model fits were observed when estimating AGB_{grass} ($r^2 = 0.42$) than estimates of AGB_{total} ($r^2 = 0.32$). However, these regressions were not particularly significant (AGB_{total} $p = 0.0683$ and AGB_{grass} $p = 0.0300$).

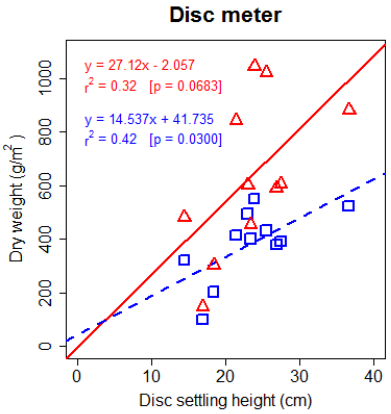

Figure 13. Ordinary Least Squares (OLS) regressions of AGB_{total} (red triangles) and AGB_{grass} (blue squares) against the disc pasture meter settling heights (cm).

The OLS regressions between TLS and SfM derived volume metrics and AGB are presented in Figure 14 for volumetric measurements using the estimated ground surface. Both TLS and SfM showed greater correspondence with AGB compared to the disc pasture meter. When estimating AGB_{total}, SfM ($r^2 = 0.74$) provided a more effective estimation than TLS ($r^2 = 0.56$). However, the smaller range of SfM volumes resulted in slopes over two and a half times more steep than TLS regressions. Removing the litter layer from AGB dry weight lowered the overall fit of each of the models, as correspondence was lower for both SfM and TLS when estimating AGB_{grass}, (SfM $r^2 = 0.51$, TLS $r^2 = 0.49$), and the fits were less significant. For both data types, the volume estimates corresponded better with AGB_{total} than with AGB_{grass} and the fits were more significant.

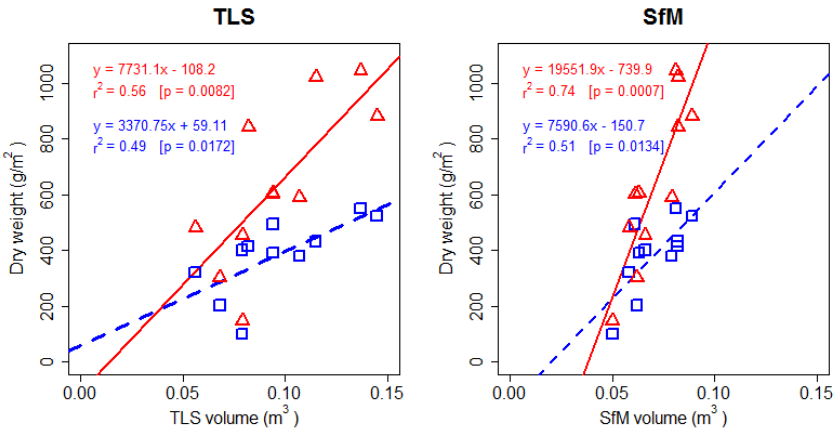

Figure 14. Ordinary Least Squares (OLS) regressions of AGB_{total} (red triangles) and AGB_{grass} (blue squares) against the TLS (left) and SfM (right) derived volume estimates (m^3) using the estimated ground surface.

The relationships between TLS and SfM derived volume using the observed ground surface and AGB are shown in the regressions presented in Figure 15. Using these observed ground surfaces, regressions of AGB_{total} against SfM ($r^2 = 0.77$) and TLS ($r^2 = 0.63$) outperform models of AGB_{total} utilizing the estimated ground surface. The same general trends observed previously using the estimated ground surface hold true with the estimated ground surface, with a noted drop in significance and model fit when assessing AGB_{grass}. In addition to the better model fits, volumes derived from the estimated ground surface tended to be greater than those derived from the observed ground surface. The mean TLS volume was 0.0960 m^3 when using the estimated ground surface, but 0.0916 m^3 when using bare earth observations. Similarly, SfM volumes using the estimated ground surface had a mean of 0.0702 m^3 versus 0.0662 m^3 when using the bare earth observation.

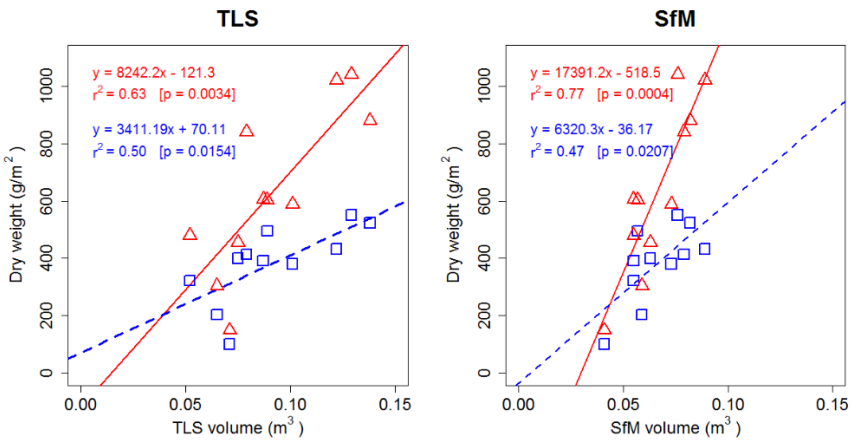

Figure 15. As Figure 14 but showing TLS (left) and SfM (right) volume estimates derived from bare earth observations rather than the estimated ground surface.

Results of the LOOCV runs (Table 1) largely corroborate with what was observed in the complete OLS regressions, and each of the 11 regressions generated using this scheme provided similar fits to those observed in Figures 13 – 15. Consequently, the same trends in r^2 and significance observed there can be observed in the LOOCV results as well. Summary statistics for each regression summarized in Tables 1 and 2 can be found in Appendix III.

Table 1. Summary statistics for the 11 LOOCV runs for TLS and SfM volume estimates using the estimated ground surface, as well as the disc pasture meter settling height. Displayed are the means and standard deviations of OLS regression F-test p-*value*, the coefficient of determination (r^2), the RMSE (g/m^2), and the residual of the 'left-out' observation (equation 2) for each regression (n=10). Additionally, $RMSE_{LOOCV}$ (g/m^2) calculated using equation 3 are presented as well. Full results of each LOOCV are found in Appendix III.

		p-value	r^2	RMSE	Residual	$RMSE_{LOOCV}$
Disc	AGB_{total}	0.089 ± 0.031	0.326 ± 0.046	223.424 ± 12.26	16.272 ± 268.20	268.70
	AGB_{grass}	0.042 ± 0.013	0.428 ± 0.040	95.955 ± 7.290	7.540 ± 119.92	120.15
TLS	AGB_{total}	0.014 ± 0.007	0.561 ± 0.054	179.987 ± 13.44	0.492 ± 219.46	219.46
	AGB_{grass}	0.027 ± 0.013	0.492 ± 0.063	90.591 ± 10.368	-0.227 ± 107.68	107.68
SfM	AGB_{total}	0.002 ± 0.001	0.740 ±0.037	138.015 ± 5.83	3.876 ± 168.68	168.73
	AGB_{grass}	0.026 ± 0.021	0.509 ± 0.086	88.306 ± 7.013	4.522 ± 111.58	111.67

Error in model prediction can be summarized through the $RMSE_{LOOCV}$ values generated by equation 1. These indicate that the disc pasture meter yielded poor predictive capability of AGB_{total}, with $RMSE_{LOOCV}$ of 268.7 g/m^2. Errors in prediction of AGB_{grass} were significantly lower at 120.25 g/m^2. These errors are quite large, however, and correspond to approximately 42% and 31 % of the mean AGB_{total} and AGB_{grass} sampled across all plots. Both TLS and SfM showed less error in estimation of AGB_{total}. SfM $RMSE_{LOOCV}$ values for AGB_{total} (168.73 g/m^2) were smaller than TLS values (219.46 g/m^2). These errors correspond to 26 and 35 % of the mean destructively sampled AGB_{total}.

In estimation of AGB_{grass}, lower and more uniform $RMSE_{LOOCV}$ values were observed for all methods. Direct comparison of these RMSE values to those of AGB_{total} models can be misleading however, and the lower values can largely be attributed to the smaller range of AGB in regressions with litter removed rather than an indication of lower accuracy in AGB_{total} models.

Table 2. As Table 1 but showing regressions using the observed ground surface in volumetric calculations rather than the estimated ground surface.

		p-value	r^2	RMSE	Residual	$RMSE_{LOOCV}$
TLS	AGB_{total}	0.006 ± 0.003	0.637 ± 0.051	163.569 ± 12.69	-0.776 ± 203.05	203.05
	AGB_{grass}	0.024 ± 0.011	0.502 ± 0.053	89.623 ± 9.196	0.348 ± 107.67	107.67
SfM	AGB_{total}	0.001 ± 0.001	0.769 ± 0.42	130.120 ± 8.40	0.728 ± 151.55	151.56
	AGB_{grass}	0.039 ± 0.040	0.463 ± 0.091	92.294 ± 5.911	7.960 ± 119.58	119.84

6.0 DISCUSSION

6.1 AGB Estimation

6.1.1 Point Cloud Generation

Point cloud generation between TLS and SfM data capture methodologies were markedly different for this grassland ecosystem. Point cloud densities varied greatly between the two, with SfM producing many more points and consequently a more detailed perspective of grass structure within the plot. The lower TLS point densities observed were largely due to the relatively large angular step of the TLS unit used (section 4.2.4).

One of the most notable differences between TLS and SfM point clouds was in the observed height of the vegetation canopy, with SfM producing much lower grass heights, and consequently volumes, than TLS (Figure 9). This underestimation of grass height comes from an apparent failure to model the extremities of fine scale vegetation (i.e. single grass blades and seed heads). This has been noted when modeling other fine scale vegetation structures such as small branches (Miller et al. 2015; Morgenroth and Gomez 2014) and the upper portions of shrubs (Hesse 2014). The difficulty in modeling these fine scale has been attributed to insufficient point cloud resolution either from camera specifications or distance to the reconstructed object (Miller et al. 2015). While this was likely a factor, very close ranges (<2m) and high camera resolution (20 Megapixels) used in this study make this unlikely to be the only explanation. Rather, the possibility of slight movement of these fine scale objects between photographs make tie point identification difficult, resulting in an increased likelihood of point identification errors and subsequent failure of proper photograph alignment and point cloud generation.

In this study, the problem was particularly pronounced with seed heads, which SfM almost always failed to model entirely.

The high degree of homogeneity of the grasses further made identifying unique points within the grass stand more difficult. SfM relies on automated identification of unique points from different camera angles to generate 3D information. However, there is very little variation between blades of grass which may be used in identifying unique points. Like vegetation movement, this can result in poor photo alignment and point cloud generation of the vegetation less accurate (Nouwakpo et al. 2015). Uniquely painted cubes placed on the corners of the plot were found to help with photo alignment, but even with these aides, point cloud modeling of the grasses lost much of the finer details of the grass structure.

Lighting conditions can also play a role in the accuracy of SfM point cloud generation (Miller et al. 2015). The consistency of lighting between photographs is incredibly important as variable lighting can lead to poor photograph alignment. It has been suggested that diffuse lighting (i.e. cloudy days) is preferred to reduce shadows and overexposure (Miller et al. 2015). However, overcast days could result in underexposed photographs, particularly when using hand held cameras, which require relatively high shutter speeds to capture crisp photographs. When light is limited, the ISO or aperture settings must therefore be changed accordingly, possibly reducing image quality. Furthermore, extremely long shutter speeds (e.g., with tripod mounted cameras) increase the likelihood of photo blur from moving grasses while the photo is being captured.

The various challenges in SfM point cloud generation observed in grasses resulted in excessively noisy point clouds. These error prone points were removed from the point

cloud using a built in depth filtering mechanism within Agisoft Photoscan. While this has been found to over smooth vegetation and lead to underestimation of vegetation height (Hesse 2014), disabling the filter entirely resulted in excessive noise that rendered analysis of the point cloud impractical. The depth filtering used was therefore minimized, but not disabled.

TLS and SfM point clouds also displayed markedly different levels of noise in the datasets. The high degree of noise TLS point clouds resulted from both the TLS sensor canopy properties of the grasses. The TLS sensor used produced relatively low point cloud densities, with pulses were sensed every 0.80 to 1.22 cm at the distances observed in this study (section 4.2.2). This is much larger than the individual grass blades, meaning that it is not possible to distinguish grass canopy structure at fine scales. Furthermore, the grass canopy is not homogenous and contains many gaps and void dispersed between the fine scale grasses. Because of this, TLS point returns were observed for both the top of the grass canopy as well as points lower in the grass stand that were detected by TLS returns due to these voids.

Another possible noise contributing factor could be from the scanning geometries used. Scan locations above the vegetation canopy have been shown to overestimate vegetation height (Ehlert and Heisig 2013). This overestimation was found to be larger at greater scanning distances. Due to the multi scan symmetry of this study, this would cause both high and low height estimations at the plot edges once all four scans have been merged. Given the range of this study however, the effect of this was likely minimal.

Alignment of the point clouds is another potential source of error in the assessment of TLS and SfM point clouds. The upper limit of scan alignment accuracy is limited largely to point cloud density, as the point cloud density determines the precision with which alignment targets can be resolved. In the context of this study, that means that alignment accuracy was limited to the resolution and accuracy of the CBL unit. Average alignment RMS error for TLS point clouds was 1.42 cm. This roughly corresponds to the point dispersal at the target locations, which ranged from 0.80 to 1.22 cm for each scan. Alignment of the SfM point clouds to the TLS point clouds showed similar alignment error with an average of 1.43 cm.

6.1.2 Sensitivity to cell size

Neither TLS nor SfM were found to be sensitive to cell size when estimating volume provided that the cells were of a sufficient size to ensure that no cells were left empty for the given point cloud densities. This sensitivity however is based on the combined relationship between the point clouds generated and the specific structural properties of the grass plots in the study, and may vary with different instrumentation or grass structure. The observed insensitivity of either technique to cell size implies that using simple height metrics (e.g., Eitel et al. 2014), at least up to 0.44 x 0.44 m plot sizes for the grasses considered in this study, is sufficient for calculating AGB in grasslands.

6.1.3 TLS and SfM AGB estimation

Results from this analysis show that both TLS and SfM are able to estimate AGB with a reasonable amount of accuracy. Robust allometric relationships are difficult to establish and require much more robust sampling (e.g., Trollope et al. 1999) than the 11 plots analyzed here. As a result, the allometric relations observed in this study were less

successful than some observed in the literature, both in terms of regression fit and overall error in predicting AGB. However, from this assessment the potential of both of these techniques can be seen. Results from both methods show relatively high predictive errors when estimating AGB_{total}, but biomass estimates showed significant errors, with errors in prediction ranging from 107 g/m^2 to 219 g/m^2. This is a substantial level of error given the range of measured AGB was 149 g/m^2 to 1043 g/m^2. Nevertheless, both TLS and SfM showed high correspondence to AGB_{total} ($r^2 = 0.56$ and $r^2 = 0.74$). These correspondences are comparable in magnitude to previous results estimating grass biomass from point cloud metrics (Eitel et al. 2014; Schaefer and Lamb 2016).

Both TLS and SfM have proven their potential for grassland vegetation assessment. While higher r^2 and lower RMSE would seem to suggest SfM would be the preferred method for grassland assessment, the tendency observed in SfM for under modeling grass height could prove to be problematic. Volume estimates for SfM in this study fell within a more narrow range than TLS volume estimates did, resulting in a much steeper OLS regression slope observed in SfM regressions. Consequently, the same error in SfM volume estimation could create a disproportionately larger effect in AGB estimation when compared to the effects the same magnitude of error in TLS volume estimation. Given that the errors in grass volume estimates of both methods may be substantial, this could prove detrimental to the selection of SfM over TLS.

6.1.4 Disc pasture meter AGB estimation

Both TLS and SfM outperformed the conventional disc pasture meter, further demonstrating their utility in AGB estimation. However, I note that the AGB estimations using the disc pasture meter fell well short of the upper limits observed in the literature,

where r^2 values greater than 0.95 have been found (Santillan et al. 1979; Karl and Nicholson 1987). However, AGB estimation of grass AGB has been shown to be greatly reduced by the presence of a significant litter layer and variable microtopography (Karl and Nicholson 1987), as well as in tall grasses (Santillan et al. 1979; Douglas and Crawford 1994). As variable litter layer and microtopography have been shown to negatively impact TLS and SfM estimates of AGB as well, it is possible that future work assessing AGB assessments in grassland systems unaffected by these variables will show better results for all three methods.

6.1.5 Effects of litter on AGB estimation

The disc pasture meter saw improvements to estimation of grass AGB with the litter layer removed, with an r^2 of 0.32 for AGB_{total} and an r^2 of 0.42 for AGB_{grass}. However, these r^2 values were still lower than r^2 using TLS or SfM for either AGB_{total} or AGB_{grass}, and all disc pasture meter regressions were much less significant than TLS or SfM.

AGB estimation using SfM or TLS volume metrics showed significant decreases in model fit when the litter layer is removed. Reduction in regression fit for AGB_{grass} data likely resulted from the inability of TLS or SfM to resolve the litter layer. Proportions of accumulated litter were highly variable, accounting for 14 % to 137 % of the grass AGB, and there was a strong relationship between the AGB_{grass} and litter (Figure 8) with larger litter proportions observed in plots with higher grass AGB. Furthermore, plots with higher AGB_{grass} tended to have larger estimated volumes (Figure 12). Because of these correlations, removing the litter weight resulted in a greater loss of AGB in plots with higher volumes. As volume estimates couldn't change to compensate

for litter removal, this resulted in a flattening of regression slopes (Figure 14). As the relationship between litter and grass biomass appears to be somewhat non-linear (Figure 8), this transformation of the data resulted in poorer regression fits.

Beyond this statistical explanation lies the complex and non-linear relationship between litter accumulation and AGB observed which can be difficult to determine (Xiong and Nilsson 1999, Knapp and Seastedt 1986). Litter decomposition rates in grasslands tends to be very low due to relatively dry conditions and low nutrient quality of many grasses (Koelling and Kucera 1965), resulting in substantial litter accumulation in undisturbed grasslands (Weaver and Rowland 1952) as was observed in this project.

Litter can influence AGB in grasslands in numerous, and sometimes competing ways. In undisturbed grasslands such as this, litter accumulation has been found to largely reduce grass productivity and therefore AGB. For example, high litter accumulation blocks sunlight from the soil surface, reducing the amount of energy available to emerging vegetation, resulting in lower productivity and lower grass shoot densities (Hulbert 1969, Knapp and Seastedt 1986). However, a large litter layer has also been shown to increase soil water content, which can decrease water stress and increase grass productivity in semiarid and water limited grass systems (Redmann 1978). By removing the litter layer from the assessment, I removed a portion of the AGB that both directly and indirectly affects the quantity and quality of standing AGB in ways that cannot be accounted for using TLS or SfM. The poor regression results observed in TLS and SfM AGB estimation when the litter weight was removed from analysis demonstrate the importance of this relationship.

While the disc pasture meter did see improvements in AGB estimation with the litter layer removed, the regression itself was still less significant that TLS or SfM estimates. Furthermore, the litter layer resided at the bottom of the grass stems and so had little influence on the grass mechanical strength and consequently on the disc settling height. This inconsistency demonstrates the difficulty in accounting for a variable litter layer using allometric relationships of AGB. While the litter layer in grassland ecosystems is an important component of AGB, the failure of TLS and SfM to account for this variation remains a methodological shortcoming. However, the relatively high performance of AGB_{total} estimation indicates that these methods can still be usefull in assessing AGB of undisturbed grasses and use in managed grassland systems would not be subject to these errors. Furthermore, an inability to account for a variable litter layer is not unique to these methods, and has been shown here and elsewhere to negatively affect other allometric methods, including the disc pasture meter (Karl and Nicholson 1987).

6.1.6 Effects of plot microtopography on AGB estimation

Further uncertainty in both TLS and SfM volume estimates resulted from the microtopography at each site. The relationships between AGB and volume using an estimated ground surface in lieu of the observed ground surface showed both lower regression fits and higher errors compared to when the observed ground surface was used. This suggests that while the estimated ground surface is able to approximate the general surface of the ground correctly, the actual ground surface was observed to contain numerous small depressions and protuberances which can cause error in volumetric measurements when the estimated ground surface was used.

At times, however, it may be necessary to use an estimated ground surface in order to preserve the nondestructive nature of the TLS and SfM biomass estimates. While this has been shown to be less accurate than using observed ground surfaces, it can still provide useful and reasonably accurate estimates of AGB despite ignoring microtopographical variation between and within plots when measuring volume. Future studies investigating AGB loss (e.g., from burning or harvesting) could avoid this problem by replacing the estimated ground surface with TLS and SfM measurements collected after the AGB event.

6.2 Practical Limitations

In choosing a method for rapid AGB estimation on grasslands, practical limitations need to be identified, and the different AGB estimation methods considered in this study have quite different practical limitations. In this respect, the rapidity of each method is a key concern.

The disc pasture meter was the quickest method, taking only seconds to collect a reading. It was simple to implement, and was the least expensive. However, it was also found to be the least accurate method for estimating AGB in this grassland. Data capture for both TLS and SfM were both relatively rapid. Using the CBL unit, TLS scanning took less than 10 minutes to set up and complete all four plot scans, with a similar amount of time required for SfM photo capture of approximately 150 photographs. Processing times for these two methods were very different. All four TLS point clouds for a given plot could be aligned and clipped to the proper extent in under 30 minutes.

Point cloud generation using SfM took over five times as long on account of the higher processing needs.

These times are largely reflected by the specifications of the instruments used for data collection and processing. The CBL unit used was built for rapid scanning and high portability (Paynter et al. 2016), and doesn't require a high performance computer to generate point clouds. SfM processing times are largely dependent on the number of input photographs and computing power. While photographic overlap was maximized for this project, further investigation is needed into determining the optimal balance of processing time and point cloud generation.

Beyond data collection and processing times, a major limitation of TLS and SfM application is vegetation movement during data acquisition, which can greatly reduce their ability to reconstruct accurate point clouds. When aligning multiple LiDAR scans, any portion of the vegetation that has moved between the scans will occupy different relative locations in each scan. This results in a localized misalignment and an overrepresentation of these portions of vegetation, adding to the noise in TLS datasets. Seed heads, protruding well above the rest of the grass canopy and being more prone to movement, are particularly culpable in adding noise to TLS point clouds. Movement of vegetation between photographs for SfM point cloud generation would result in photograph misalignment due to changing relative locations of the vegetation within each photograph.

Because of this, wind is a key factor in point cloud generation using both of these techniques as well. While study design limited the effect of wind in this assessment, grasses are prone to movement in even light winds. Depending on the climatic

conditions of the study site, this can severely limit the number of sites visited, as was the case with this study. As investigators would ideally need to wait for windless days, the limited time frame of a field season is restricted even further. This can greatly reduce the predictive power of allometric relationships generated. So while direct effects of wind on the data were minimized, reduced sampling ability meant that wind still limited the results in that fewer replicates were available to generate robust allometric relationships. The disc pasture meter is not prone to such wind induced errors,

Further investigation is needed into the precise effects of wind on TLS and SfM point cloud modeling of grasslands. While failure of photographic alignment will likely limit SfM data acquisition, it is possible that TLS will not be as adversely affected. Under light or moderate winds, while grasses will invariably move, overall grass height will vary relatively little. This decreases the precision of point cloud generation, particularly between multiple scans. However, given the relative insensitivity observed in this study of volume estimation to cell size used, this added noise may prove to be irrelevant in AGB estimation.

Several reasons for errors AGB estimation using TLS and SfM have been discussed previously and primarily occur in the generation of the point clouds. However, it is prudent to discuss the basic assumptions the volumetric assessment employed here. Grass stand structure can be very complex, and the generated point clouds indicate that this complexity cannot be captured by TLS or SfM, at least with the instruments being used and the structure of the grasses being investigated. While using more advanced and higher resolution instruments could potentially alleviate some of these errors through resolving finer details of the grass structure, the underlying assumption is that the volume

of standing grass is directly related to AGB. While this may be a reasonable assumption, it is worthwhile to discuss how it impacts AGB estimation using the methodologies presented here.

This study's volumetric assessment assumes that the entire area under the measured grass height contributes to the plot biomass. With the resolution of data available for this study, it is impossible to resolve individual grass blades, meaning that the precise grass structure cannot be resolved. Even if individual grasses could be resolved, occlusion of lower portions of the grass stand would still occur from the upper portions of the grass canopy, making observations of these lower sections impossible. Grass stands contain numerous voids between the individual plants, and given that many of these voids cannot be directly measured by TLS or SfM, it is impossible to verify their true structure with this methodology. Consequently, TLS and SfM inherently overestimate grass volume, as the volumes of both the grasses and the voids are included in their volume metrics. The implicit assumption therefore is that these voids occur in a regular manner such that the volume of the entire grass stand, including vegetation as well as voids, can be linearly related to AGB.

Given that this study only investigates homogenous stands of Smooth Brome at the same life cycle stages and in the same environment, this is a reasonable assumption to make. However, extrapolating these results to different and more complex conditions is challenging, and as with other allometric techniques for AGB estimation, it will require extensive calibration and assessment.

6.3 Future Applications

Further work is needed to assess the impact of confounding factors of AGB estimation using SfM or TLS derived measurements. Such factors may include grass species composition, growth stage, structure and condition, variable litter, the effects of wind, and seasonality. Further work to determine the major influencing factors and to establish optimal configuration and instrumentation for SfM and TLS data acquisition is suggested. Additionally, both SfM and TLS can potentially be used in the classification of dead versus living vegetation using the red, green, and blue radiance values generated by SfM or the return intensity of TLS.

Differences in measurement of grass volume and subsequently AGB estimation opens the possibility for using the two methods in conjunction to estimate AGB either through linear regression between multiple SfM and TLS point cloud metrics (e.g., volume), or by merging the two point clouds and generating point cloud metrics from this new combined point cloud. By combining SfM and TLS derived vegetation metrics, it is possible that more accurate AGB estimation could be obtained.

Perhaps the greatest opportunities both of these technologies hold is in their potential for upscaling AGB estimates from plot-level measurements investigated in this study to direct field-level measurements, such as with terrestrial vehicle mounted instruments or merging scans from multiple adjacent locations to assess a larger spatial extent. Additionally, given the relatively high point density and low spatial error of SfM and TLS point clouds, they can be used to calibrate and validate point clouds generated from airborne or spaceborne platforms (Greaves et al. 2017). This can be used to help

assess studies a much larger spatial scales, for example in global analysis using platforms such as the upcoming Global Ecosystem Dynamics Investigation (GEDI) LiDAR.

The systematic collection of SfM or TLS data across larger spatial extents could provide a great advantage over the disc pasture meter, which is limited to plot-level assessments. Studies of AGB loss using these techniques are particularly promising, as direct measurements of a ground surface become possible allowing for more reliable volumetric measurements.

7.0 CONCLUSIONS

The results of this study demonstrated the potential of Structure-from-Motion (SfM) photogrammetry and Terrestrial Laser Scanning (TLS) for nondestructive estimation of grass aboveground biomass (AGB) in a prairie grassland in South Dakota. Volume metrics extracted from the SfM and TLS 3D point clouds, and also conventional disc pasture meter settling heights, were compared to destructively harvested AGB total (grass and litter) and AGB grass plot measurements at 11 sites. The three approaches were assessed based on the OLS regression coefficient of determination (r^2), and the root mean squared error (RMSE) derived from a leave-one-out cross validation scheme (Section 4.5).

The four thesis questions (Section 2.0) were all addressed and the findings for each are summarized briefly below.

Q1) How accurately can the SfM approach estimate aboveground grass biomass?
SfM provided the most accurate results of the three approaches investigated with an r^2 of 0.74 and an RMSE of 169 g/m^2 for AGB_{total}.

Q2) How accurately can the TLS approach estimate aboveground grass biomass?
TLS was less accurate than SfM with an r^2 of 0.56 and an RMSE of 219 g/m^2 for AGB_{total}.

Q3) Are the remote sensing approaches (SfM and TLS) more accurate than the conventional disc pasture meter approach?

The SfM and TLS approaches were more accurate than the conventional disc pasture meter approach that provided an r^2 of 0.32 and a RMSE of 269 g/m^2 for AGB_{total}. The disc pasture meter was less effective than in certain other studies reported in the literature however (which may be due to site and grass differences).

Q4) What are the limitations of each approach (SfM, TLS, and disc pasture meter) for rapid field based assessments of aboveground grass biomass?

Each approach had limitations. The SfM andTLS approaches were not able to penetrate the entirety of the grass canopy. Consequently, the SfM and TLS volume estimates had higher correspondence with AGB_{total} (r^2 = 0.74 and r^2 = 0.56) than with AGB_{grass} (r^2 = 0.51 and r^2 = 0.49). In other vegetation canopies this may not be the case. The disc pasture meter approach is straightforward and rapid as it takes only seconds to place and measure the disc settling height. Unlike the TLS and SfM approaches it can be undertaken on windy days and does not require consistent solar illumination conditions needed for effective SfM point cloud generation. The CBL used in this thesis is a new generation of TLS that is optimized for rapid scanning and portability. It took less than 10 minutes to set up and complete the four CBL scans for each plot. A similar amount of time was spent taking the approximately 150 digital photographs per plot needed for the SfM approach. However, the processing required to generate 3D point clouds was markedly different between the TLS and SfM approaches, typically 30 minutes per plot

for the TLS data and five times more for the SfM data due to greater computer processing requirements. The disc pasture meter is the least expensive of the three approaches. Although the CBL is more expensive than a digital camera it does not require a high performance computer to process the collected data. The TLS processing could be undertaken on a laptop computer in the field but except for generating "quick look" images this was not considered an advantage due to the difficulty of operating a laptop in natural daylight.

In summary, both the SfM and TLS approaches demonstrated their potential and enabled grass AGB estimation with greater accuracy than the conventional disc pasture meter approach. Each approach has different limitations, and the results of this thesis suggest that the selection of a particular approach should consider accuracy and practical application requirements. Further research to determine the major influencing factors and to establish optimal methodologies for SfM and TLS data acquisition in grassland ecosystems is also suggested.

REFERENCES

Agisoft LLC. 2016. Agisoft photoscan professional edition. Agisoft LLC: St Petersburg.

Andújar, D, A. Escolà, J. Rosell-Polo, C. Fernández-Quintanilla, and J. Dorado. 2013. Potential of a terrestrial LiDAR-based system to characterise weed vegetation in maize crops. *Computers and Electronics in Agriculture* 92:11-15.

Boyda, E. D. (2013). Evaluation of the reference unit method for herbaceous biomass estimation in native grasslands of southwestern South Dakota (Unpublished master's thesis). South Dakota State University, Brookings, SD.

Bransby, D. I., A. G. Matches, and G. F. Krause. 1977. Disk meter for rapid estimation of herbage yield in grazing trials." *Agronomy Journal* 69(3):393-396.

Briggs, J. M., and A. K. Knapp. 1995. Interannual variability in primary production in tallgrass prairie: climate, soil moisture, topographic position, and fire as determinants of aboveground biomass. *American Journal of Botany* 82:1024-1030.

Calders, K., J. Armston, G. Newnham, M. Herold, and N. Goodwin. 2014. Implications of sensor configuration and topography on vertical plant profiles derived from terrestrial LiDAR. *Agricultural and Forest Meteorology* 194:104-117.

Calders, K., G. Newnham, A. Burt, S. Murphy, P. Raumonen, M. Herold, D. Culvenor… et al. 2015. Nondestructive estimates of above-ground biomass using terrestrial laser scanning. *Methods in Ecology and Evolution* 6(2):198-208.

Carlyle, C. N., L. H. Fraser, C. M. Haddow, B. A. Bings, and W. Harrower. 2010. The use of digital photos to assess visual cover for wildlife in rangelands. *Journal of Environmental Management* 91(6):1366-1370.

Chave, J., C. Andalo, S. Brown, M. A. Cairns, J. Q. Chambers, D. Eamus, H. Fölster et al. 2005. Tree allometry and improved estimation of carbon stocks and balance in tropical forests. *Oecologia* 145(1):87-99.

CloudCompare. (2016). GPL software version 2.7. Retrieved from http://www.cloudcompare.org

Costanza, R., R. d'Arge, R. de Groot, S. Faber, M. Grasso, B. Hannon, K. Limburg… et al. 1997. The value of the world's ecosystem services and natural capital. *Nature* 387(): 253-260.

Coveney, S., and A. S. Fotheringham. 2011. Terrestrial laser scan error in the presence of dense ground vegetation. *The Photogrammetric Record* 26(135):307-324.

Dokken, D. A., and L. C. Hulbert. 1976. Effect of standing dead plants on stem density in bluestem prairie. In *Fifth Midwest Prairie Conference*, Iowa State University, Ames. 78-81.

Douglas, J. T., and C. E. Crawford. 1994. An evaluation of the drop-disc technique for measurements of herbage production in ryegrass for silage. *Grass and Forage Science* 49:252

Ehlert, D., and M. Heisig. 2013. Sources of angle-dependent errors in terrestrial laser scanner-based crop stand measurement. *Computers and electronics in agriculture* 93:10-16.

Eisfelder, C., C. Kuenzer, and S. Dech. 2012. Derivation of biomass information for semi-arid areas using remote-sensing data. *International Journal of Remote Sensing* 33(9):2937-2984.

Eitel, J. U. H., T. S. Magney, L. A. Vierling, T. T. Brown, and D. R. Huggins. 2014. LiDAR based biomass and crop nitrogen estimates for rapid, non-destructive assessment of wheat nitrogen status. *Field Crops Research* 159: 21-32.

Erdle, K., B. Mistele, and U. Schmidhalter. 2011. Comparison of active and passive spectral sensors in discriminating biomass parameters and nitrogen status in wheat cultivars. *Field Crops Research* 124(1):74-84.

Fan, L., W. Powrie, J. Smethurst, P. M. Atkinson, and H. Einstein. 2014. The effect of short ground vegetation on terrestrial laser scans at a local scale. *ISPRS Journal of Photogrammetry and Remote Sensing* 95:42-52.

Flombaum, P., and O. Sala. 2007. A non-destructive and rapid method to estimate biomass and aboveground net primary production in arid environments. *Journal of Arid Environments* 69(2):352-358.

FAO. 2012. Food and Agriculture Organization of the United Nations. FRA 2015 terms and definitions (Forest Resource Assessment Working Paper 180). Rome, Italy.

Grau, E., S. Durrieu, R. Fournier, J. Gastellu-Etchegorry, and T. Yin. 2017. Estimation of 3D vegetation density with Terrestrial Laser Scanning data using voxels. A sensitivity analysis of influencing parameters. Remote Sensing of Environment 191:373-388.

Greaves, H. E., L. A. Vierling, J. U. H. Eitel, N. T. Boelman, T. S. Magney, C. M. Prager, and K. L. Griffin. 2015. Estimating aboveground biomass and leaf area of low-stature Arctic shrubs with terrestrial LiDAR. *Remote Sensing of Environment* 164:26-35.

Greaves, H. E., L. A. Vierling, J. U. H. Eitel, N. T. Boelman, T. S. Magney, C. M. Prager, and K. L. Griffin. 2017. Applying terrestrial lidar for evaluation and calibration of airborne lidar-derived shrub biomass estimates in Arctic tundra. *Remote Sensing Letters* 8(2):175-184.

Guarnieri, A., A. Vettore, F. Pirotti, M. Menenti, and M. Marani. 2009. Retrieval of small-relief marsh morphology from terrestrial laser scanner, optimal spatial filtering, and laser return intensity. *Geomorphology* 113(1):12-20.

Harmoney, K. R., K. J. Moore, J. R. George, E. C. Brummer, and J. R. Russell. 1997. Determination of pasture biomass using four indirect methods." *Agronomy Journal* 89(4):665-672.

Haydock, K. P., and N. H. Shaw. 1975. The comparative yield method for estimating dry matter yield of pasture. Animal Production Science 15(76):663-670.

Hesse, R. 2014. Three-dimensional vegetation structure of Tillandsia latifolia on a coppice dune. *Journal of Arid Environments* 109:23-30.

Holmes, C. 1974. The Massey grass meter. *Dairy Farming Annual*. Palmerston North, New Zealand: Massey University. 26-30.

Hosoi, F., and K. Omasa. 2006. Voxel-based 3-D modeling of individual trees for estimating leaf area density using high-resolution portable scanning lidar. *IEEE Transactions on Geoscience and Remote Sensing* 44(12):3610-3618.

Hosoi, F., and K. Omasa. 2009. Estimating vertical plant area density profile and growth parameters of a wheat canopy at different growth stages using three-dimensional portable lidar imaging. *ISPRS Journal of Photogrammetry and Remote Sensing* 64(2):151-158.

Hosoi, F., Y. Nakai, and K. Omasa. 2013. 3-D voxel-based solid modeling of a broad-leaved tree for accurate volume estimation using portable scanning lidar. *ISPRS Journal of Photogrammetry and Remote Sensing* 82:41-48.

Hulbert, L. C. 1969. Fire and litter effects in undisturbed bluestem prairie in Kansas. *Ecology* 50(5):874-877.

James, M. R., and Stuart Robson. 2012. Straightforward reconstruction of 3D surfaces and topography with a camera: Accuracy and geoscience application. *Journal of Geophysical Research: Earth Surface* 117(F3):1-24.

Kankare, V., M. Holopainen, M. Vastaranta, E. Puttonen, X. Yu, J. Hyyppä, M. Vaaja, H. Hyyppä, and P. Alho. 2013. Individual tree biomass estimation using terrestrial laser scanning. *ISPRS Journal of Photogrammetry and Remote Sensing* 75:64-75.

Karl, M. G., and R. A. Nicholson. 1987. Evaluation of the forage-disk method in mixed-grass rangelands of Kansas. *Journal of Range Management*: 467-471.

Kauffman, J. Boone, D. L. Cummings, and D. E. Ward. 1994. Relationships of fire, biomass and nutrient dynamics along a vegetation gradient in the Brazilian cerrado. *Journal of Ecology* 82(3): 519-531.

Kelbe, D., P. Romanczyk, J. van Aardt, and K. Cawse-Nicholson. 2013. Reconstruction of 3D tree stem models from low-cost terrestrial laser scanner data. SPIE Defense, Security, and Sensing: 873106-873106.

Kirmse, R. D., and B. E. Norton. 1985. Comparison of the reference unit method and dimensional analysis methods for two large shrubby species in the Caatinga woodlands. *Journal of Range Management* 38(5):425-428.

Knapp, A. K., and T. R. Seastedt. 1986. Detritus accumulation limits productivity of tallgrass prairie. *BioScience* 36(10): 662-668.

Knapp, A. K., and M. D. Smith. 2001. Variation among biomes in temporal dynamics of aboveground primary production. *Science* 291(5503): 481-484.

Koelling, M. R., and C. L. Kucera. 1965. Dry matter losses and mineral leaching in bluestem standing crop and litter. *Ecology* 46(4):529-532.

Lamond, R. E., J. O. Fritz, and P. D. Ohlenbusch. 1992. Smooth Brome Production and Utilization. Kansas State University Cooperative Extension Services. November 1992.

Li, A., N. F. Glenn, P. J. Olsoy, J. J. Mitchell, and R. Shrestha. 2015. Aboveground biomass estimates of sagebrush using terrestrial and airborne LiDAR data in a dryland ecosystem. *Agricultural and Forest Meteorology* 213:138-147.

Liang, X., A. Jaakkola, Y. Wang, J. Hyyppä, E. Honkavaara, J. Liu, and H. Kaartinen. 2014. The use of a hand-held camera for individual tree 3D mapping in forest sample plots. *Remote Sensing* 6(7):6587-6603.

Liang, X., Y. Wang, A. Jaakkola, A. Kukko, H. Kaartinen, J. Hyyppa, E. Honkavaara, and J. Liu. 2015. Forest Data Collection Using Terrestrial Image-Based Point Clouds From a Handheld Camera Compared to Terrestrial and Personal Laser Scanning. *IEEE Transactions on Geoscience and Remote Sensing* 53(9):5117-5132.

Loreau, M., and Hector, A. (2001). Partitioning selection and complementarity in biodiversity experiments. *Nature*, 412(6842), 72-76.

Loudermilk, E. L., J. K. Hiers, J. J. O'Brien, R. J. Mitchell, A. Singhania, J. C. Fernandez, W. P. Cropper, and K. C. Slatton. 2009. Ground-based LIDAR: a novel approach to quantify fine-scale fuelbed characteristics. *International Journal of Wildland Fire* 18(6):676-685.

Mannetje, L. 2000. "Measuring biomass of grassland vegetation." In *Field and Laboratory Methods for Grassland and Animal Production Research*. 2000, edited by L. 't Mannetje and R. M. Jones, 151-177. Wallingford, Oxon, U.K.: CABI Publishing.

McNaughton, S. J. 1985. Ecology of a grazing ecosystem: the Serengeti. *Ecological Monographs* 55(3): 259-294.

Miller, J., J. Morgenroth, and C. Gomez. 2015. 3D modelling of individual trees using a handheld camera: Accuracy of height, diameter and volume estimates. *Urban Forestry & Urban Greening* 14(4):932-940.

Morgenroth, J., and C. Gomez. 2014. Assessment of tree structure using a 3D image analysis technique—A proof of concept. *Urban Forestry & Urban Greening* 13(1):198-203.

Nogueira, E. M., B. W. Nelson, and P. M. Fearnside. 2006. Volume and biomass of trees in central Amazonia: influence of irregularly shaped and hollow trunks. *Forest Ecology and Management* 227(1):14-21.

Nouwakpo, S. K., M. A. Weltz, and K. McGwire. 2015. Assessing the performance of structure-from-motion photogrammetry and terrestrial LiDAR for reconstructing soil surface microtopography of naturally vegetated plots. *Earth Surface Processes and Landforms* 41(3)

Olsoy, P. J., N. F. Glenn, and P. E. Clark. 2014a. Estimating sagebrush biomass using terrestrial laser scanning. *Rangeland Ecology & Management* 67(2):224-228.

Olsoy, P. J., N. F. Glenn, P. E. Clark, and D. R. Derryberry. 2014b. Aboveground total and green biomass of dryland shrub derived from terrestrial laser scanning. *ISPRS Journal of Photogrammetry and Remote Sensing* 88:166-173.

Owensby, C. E., P. I. Coyne, J. M. Ham, L. M. Auen, and A. K. Knapp. 1993. Biomass Production in a Tallgrass Prairie Ecosystem Exposed to Ambient and Elevated CO2. *Bulletin of the Ecological Society of America* 3(4):644-653.

Özçelik, R., H. V. Wiant, and J. R. Brooks. 2008. Accuracy using xylometry of log volume estimates for two tree species in Turkey. *Scandinavian Journal of Forest Research* 23(3):272-277.

Paynter, I., E. Saenz, D. Genest, F. Peri, A. Erb, Z. Li, K. Wiggin, J. Muir, P. Raumonen, E. Schaaf, A. Strahler, and C. Schaaf. 2016. "Observing ecosystems with lightweight, rapid-scanning terrestrial lidar scanners." *Remote Sensing in Ecology and Conservation* 2(4):174-189.

Radtke, P. J., H. T. Boland, and G. Scaglia. 2010. An evaluation of overhead laser scanning to estimate herbage removals in pasture quadrats. *Agricultural and forest meteorology* 150(12):1523-1528.

Raumonen, P., M. Kaasalainen, M. Åkerblom, S. Kaasalainen, H. Kaartinen, M. Vastaranta, M. Holopainen, M. Disney, and P. Lewis. 2013. Fast automatic precision tree models from terrestrial laser scanner data. *Remote Sensing* 5(2):491-520.

Rayburn, E. 1997. An acrylic plastic weight plate for estimating forage yield. West Virginia University Extension Service. http://anr.ext.wvu.edu/r/download/195123. Accessed July 17, 2016.

Rayburn, E. B., and S. B. Rayburn. 1998. A standardized plate meter for estimating pasture mass in on-farm research trials. Agronomy Journal 90(2):238-241.

Redmann, R. E. 1978. Plant and soil water potentials following fire in a northern mixed grassland. *Journal of Range Management* 31(6):443-445.

Reppert, J. N., Meredith J. Morris, and Charles A. Graham. 1962. Estimation of herbage on California annual-type range. *Journal of Range Management* 15(6): 318-323.

Robel, R., J. N. Briggs, A. D. Dayton, and L. C. Hulbert. 1970. Relationships between visual obstruction measurements and weight of grassland vegetation. *Journal of Range Management* 23(4): 295-297.

Rowell, E., and C. Seielstad. 2012. Characterizing grass, litter, and shrub fuels in longleaf pine forest pre-and post-fire using terrestrial LiDAR. *Proceedings of SilviLaser*: 16-19.

Sah, J., M. S. Ross, S. Koptur, and J. R. Snyder. 2004. Estimating aboveground biomass of broadleaved woody plants in the understory of Florida Keys pine forests. *Forest Ecology and Management* 203(1):319-329.

Santillan, R. A., W. R. Ocumpaugh, and G. O. Mott. 1979. Estimating forage yield with a disk meter. *Agronomy Journal* 71(1):71-74.

Schaefer, M.l T., and D. W. Lamb. 2016. A combination of plant NDVI and LiDAR measurements improve the estimation of pasture biomass in Tall Fescue (*Festuca arundinacea* var. Fletcher). *Remote Sensing* 8(2):109.

Schori, F., A. Pol-van Dasselaar, H. F. M. Aarts, A. de Vliegher, A. Elgersma, D. Reheul, J. A. Reijneveld, J. Verloop, and A. Hopkins. 2015. Sward surface height estimation with a rising plate meter and the C-Dax Pasture meter in Grassland and forages in high output dairy farming systems. *Proceedings of the 18th Symposium of the European Grassland Federation*, Wageningen, The Netherlands, 15-17 June 2015, 310-312. Wageningen Academic Publishers.

Scurlock, J. M. O., and D. O. Hall. 1998. The global carbon sink: a grassland perspective. *Global Change Biology* 4(2):229-233.

SDSU Mesonet, South Dakota Climate and Weather. South Dakota State University. Available online at http://climate.sdstate.edu. Accessed 2/16/17.

Segura, M., and M. Kanninen. 2005. Allometric models for tree volume and total aboveground biomass in a tropical humid forest in Costa Rica. *Biotropica* 37(1):2-8.

Seielstad, C., C. Stonesifer, E. Rowell, and L. Queen. 2011. Deriving fuel mass by size class in Douglas-fir (*Pseudotsuga menziesii*) using terrestrial laser scanning. *Remote Sensing* 3(8):1691-1709.

Serrano, J. M., J. O. Peça, J. M. Da Silva, and S. Shahidian. 2011. Calibration of a capacitance probe for measurement and mapping of dry matter yield in Mediterranean pastures. *Precision Agriculture* 12(6):860-875.

Soil Survey Staff, Natural Resources Conservation Service, United States Department of Agriculture. Web Soil Survey. Available online at https://websoilsurvey.sc.egov.usda.gov/. Accessed 2/16/17.

Smith, R. J. "Use and misuse of the reduced major axis for line-fitting. 2009. *American Journal of Physical Anthropology*. 140(3): 476-486.

Ter-Mikaelian, M. T., and M. D. Korzukhin. 1997. Biomass equations for sixty-five North American tree species. *Forest Ecology and Management* 97(1):1-24.

Thormählen, T., N. Hasler, M. Wand, and H. Seidel. 2010. Registration of sub-sequence and multi-camera reconstructions for camera motion estimation." *Journal of Virtual Reality and Broadcasting* 7(2):1-10.

Tilman, D., J. Hill, and C. Lehman. "Carbon-negative biofuels from low-input high-diversity grassland biomass." *Science* 314.5805 (2006): 1598-1600.

Tilman, D., P. B. Reich, J. Knops, D. Wedin, T. Mielke, and C. Lehman. (2001). Diversity and productivity in a long-term grassland experiment. *Science*, *294*(5543), 843-845.

Trollope, W. S. W., L. A. Trollope, A. L. F. Potgieter, and N. Zambatis. 1996. SAFARI-92 characterization of biomass and fire behavior in the small experimental burns in the Kruger National Park. *Journal of Geophysical Research: Atmospheres* 101(D19):23531-23539.

Trotter, M. G., D. W. Lamb, G. E. Donald, and D. A. Schneider. 2010. Evaluating an active optical sensor for quantifying and mapping green herbage mass and growth in a perennial grass pasture. *Crop and Pasture Science* 61(5):389-398.

Ullman, S. 1979. The Interpretation of Structure from Motion. *Proceedings of the Royal Society of London*. Series B, Biological Sciences, 1979: 1-35.

Umphries, T. 2013. Characterizing fuelbed structure, depth, and mass in a grassland using terrestrial laser scanning. Master's thesis, University of Montana. Paper 188:1-96.

Usó, J. L., J. Mateu, T. Karjalainen, and P. Salvador. 1997. Allometric regression equations to determine aerial biomasses of Mediterranean shrubs. *Plant Ecology* 132(1):59-69.

Van der Zande, D., W. Hoet, I. Jonckheere, J. van Aardt, and P. Coppin. 2006. Influence of measurement set-up of ground-based LiDAR for derivation of tree structure. *Agricultural and Forest Meteorology* 141(2):147-160.

Vickery, P., I. L. Bennett, and G. R. Nicol. 1980. An improved electronic capacitance meter for estimating herbage mass. *Grass and Forage Science* 35(3):247-252.

Vierling, L. A., Y. Xu, J. U. H Eitel, and J. S. Oldow. 2013. Shrub characterization using terrestrial laser scanning and implications for airborne LiDAR assessment. *Canadian Journal of Remote Sensing* 38(6):709-722.

Wallace, L., V.Gupta, K. Reinke, and S. Jones. 2016. An assessment of pre-and post- fire near surface fuel hazard in an Australian dry sclerophyll forest using point cloud data captured using a terrestrial laser scanner. *Remote Sensing* 8(8):679-693.

Weaver, J. E., and N. W. Rowland. 1952. Effects of excessive natural mulch on development, yield, and structure of native grassland. *Botanical Gazette* 114(1):1-19.

Williamson, S. C., J. K. Detling, J. L. Dodd, and M. I. Dyer. 1987. Nondestructive estimation of shortgrass aerial biomass. *Journal of Range Management* 40(3):254-256.

Xiong, S., and C. Nilsson. 1999. The effects of plant litter on vegetation: a meta-analysis. *Journal of Ecology* 87(6):984-994.

Yao, T., X. Yang, F. Zhao, Z. Wang, Q. Zhang, D. Jupp, J. Lovell et al. 2011. Measuring forest structure and biomass in New England forest stands using Echidna ground-based lidar. *Remote sensing of Environment* 115(11):2965-2974.

Zambatis, N., P. J. K. Zacharias, C. D. Morris, and J. F. Derry. "Re-evaluation of the disc pasture meter calibration for the Kruger National Park, South Africa." African Journal of Range and Forage Science 23, no. 2 (2006): 85-97

Zhao, F., X. Yang, A. H. Strahler, C. L. Schaaf, T. Yao, Z. Wang, M. O. Román et al. 2013. A comparison of foliage profiles in the Sierra National Forest obtained with a full-waveform under-canopy EVI lidar system with the foliage profiles obtained with an airborne full-waveform LVIS lidar system. *Remote Sensing of Environment* 136:330-341.

APPENDICES

Appendix I: Sensor Specifications and Process Settings

LiDAR Unit	SICK LMS151
Angular Resolution	0.25°
Beam Wavelength	605 nm
Beam Divergence	0.86°
Maximum Range	40 meters
Horizontal view	360°
Vertical view	270°
Scan Time	33 seconds
Weight	3.9 kg
Camera	Canon EOS 6D
Resolution	20 MP
Lens	Canon EF 24-70mm f/4L IS USM
Server Specifications	Dell PowerEdge R815
Operating System	Linux
Processor	AMD Opteron™ Processor 6348
RAM	512 GB
PhotoScan Parameters	
Photo Alignment	
Accuracy	Low
Pair Selection	Generic
Key Point Limit	400,000
Tie Point Limit	10,000
Dense Cloud Generation	
Quality	High
Depth Filtering	Mild

Appendix II: Data

Site	AGB_{total} (g/m^2)	AGB_{grass} (g/m^2)	Disc Settling Height (cm)	TLS volume (m^3) - estimated ground	SfM volume (m^3) - estimated ground	TLS volume (m^3) - observed ground	SfM volume (m^3) - observed ground
1	148.638	99.512	16.9	0.079	0.050	0.071	0.041
2	303.032	202.877	18.4	0.068	0.062	0.065	0.059
3	479.831	321.243	14.4	0.056	0.058	0.052	0.055
4	602.731	494.565	23.0	0.094	0.061	0.089	0.057
5	455.720	400.130	23.4	0.079	0.066	0.075	0.063
6	882.114	524.035	36.7	0.145	0.089	0.138	0.082
7	1042.998	550.777	23.9	0.137	0.081	0.129	0.076
8	1023.001	432.135	25.5	0.115	0.082	0.122	0.089
9	841.211	413.812	21.4	0.082	0.082	0.079	0.079
10	605.601	391.088	27.5	0.094	0.063	0.087	0.055
11	589.431	379.511	26.9	0.107	0.079	0.101	0.073

Appendix III: LOOCV Results

Table A3.1. Results of the 11 Leave-one-out cross validation (LOOCV) regressions for each method against the AGB_{total} data (left series) and AGB_{grassl} data (right series). Displayed are the OLS regression F-test p-*value*, the coefficient of determination (r^2), the RMSE, and the residual of the 'left-out' observation for each regression (n=10).

Run	**AGB_{total} ~ TLS**			
	p-value	r^2	RMSE	residual
1	0.008	0.610	148.925	406.057
2	0.021	0.506	186.889	141.797
3	0.010	0.587	182.010	-220.832
4	0.013	0.558	191.112	17.428
5	0.015	0.542	190.524	53.779
6	0.013	0.557	183.564	218.450
7	0.033	0.451	187.957	-133.012
8	0.014	0.550	172.499	-280.711
9	0.004	0.676	159.040	-356.915
10	0.013	0.558	191.136	14.269
11	0.010	0.580	186.200	145.101

Run	**AGB_{grass} ~ TLS**			
	p-value	r^2	RMSE	residual
1	0.006	0.628	58.722	259.130
2	0.042	0.422	91.640	105.786
3	0.019	0.517	92.384	-104.506
4	0.016	0.536	88.053	-130.543
5	0.019	0.520	93.064	-85.733
6	0.043	0.420	95.952	39.818
7	0.055	0.388	95.774	-43.199
8	0.027	0.479	96.317	16.939
9	0.018	0.521	92.778	-88.606
10	0.025	0.487	96.314	-16.654
11	0.023	0.496	95.500	45.068

Run	**AGB_{total} ~ SfM**			
	p-value	r^2	RMSE	residual
1	0.005	0.644	142.182	136.346
2	0.001	0.744	134.623	195.340
3	0.001	0.744	143.273	-105.199
4	0.001	0.773	137.110	-175.341
5	0.001	0.742	142.930	105.566
6	0.001	0.745	139.322	170.998
7	0.001	0.741	129.186	-237.929
8	0.002	0.723	135.398	-193.940
9	0.002	0.726	146.185	26.851
10	0.001	0.759	141.252	-129.856
11	0.000	0.806	126.700	249.801

Run	**AGB_{grass} ~ SfM**			
	p-value	r^2	RMSE	residual
1	0.087	0.322	79.251	198.049
2	0.022	0.500	85.211	135.068
3	0.021	0.507	93.372	-38.888
4	0.002	0.703	70.420	-213.038
5	0.018	0.526	92.545	-55.546
6	0.036	0.443	94.029	1.180
7	0.029	0.470	89.134	-103.483
8	0.020	0.514	93.013	48.072
9	0.017	0.531	91.839	70.326
10	0.016	0.536	91.542	-72.586
11	0.015	0.542	91.006	80.584

Table A3.2. As Table A3.1 but for regressions calculated using the disc pasture meter settling height.

Run	AGB_{total} ~ Disc			
	p-value	r^2	RMSE	residual
1	0.167	0.224	209.972	389.046
2	0.123	0.271	227.097	231.210
3	0.091	0.316	234.168	-133.720
4	0.087	0.322	236.679	20.880
5	0.079	0.336	229.384	194.514
6	0.101	0.300	230.556	261.013
7	0.050	0.398	196.771	-436.841
8	0.077	0.340	208.961	-371.562
9	0.058	0.380	219.898	-292.939
10	0.072	0.349	232.051	159.882
11	0.073	0.347	232.126	157.507

Run	AGB_{grass} ~ Disc			
	p-value	r^2	RMSE	residual
1	0.068	0.358	77.125	237.630
2	0.059	0.376	95.211	126.793
3	0.033	0.451	98.452	-102.706
4	0.029	0.469	94.172	-130.404
5	0.041	0.425	101.867	-20.047
6	0.056	0.383	98.981	120.292
7	0.023	0.497	86.827	-177.870
8	0.043	0.418	101.834	-21.949
9	0.035	0.444	99.995	-67.948
10	0.036	0.440	100.594	58.356
11	0.036	0.442	100.447	60.789

Table A3.2. As Table A3.1 but for regressions calculated using the observed ground surface rather than the estimated ground surface for volumetric measurements.

Run	AGB_{total} ~ TLS			
	p-value	r^2	RMSE	residual
1	0.004	0.672	136.467	369.217
2	0.009	0.593	169.543	136.375
3	0.004	0.675	161.397	-244.407
4	0.006	0.634	173.938	10.535
5	0.007	0.621	173.408	47.166
6	0.006	0.639	165.579	212.482
7	0.014	0.551	169.894	-138.676
8	0.011	0.579	166.819	-175.635
9	0.001	0.752	139.120	-350.434
10	0.006	0.634	173.937	-10.799
11	0.005	0.653	169.153	135.644

Run	AGB_{grass} ~ TLS			
	p-value	r^2	RMSE	residual
1	0.009	0.591	61.573	249.179
2	0.036	0.441	90.140	108.850
3	0.017	0.529	91.230	-104.499
4	0.014	0.552	86.517	-133.078
5	0.017	0.531	91.997	-84.946
6	0.039	0.430	95.125	26.660
7	0.047	0.408	94.165	-55.770
8	0.020	0.510	93.394	68.552
9	0.017	0.529	92.052	-83.540
10	0.022	0.501	95.021	-26.708
11	0.021	0.505	94.637	39.130

Run	AGB_{total} ~ SfM			
	p-value	r^2	RMSE	residual
1	0.004	0.672	136.542	75.672
2	0.000	0.798	119.413	231.351
3	0.001	0.766	137.057	-49.304
4	0.001	0.794	130.558	-149.679
5	0.001	0.781	131.760	134.281
6	0.001	0.751	137.511	32.119
7	0.000	0.808	111.071	-277.481
8	0.002	0.713	137.786	9.459
9	0.001	0.757	137.720	17.014
10	0.000	0.810	125.223	-197.475
11	0.000	0.806	126.685	182.050

Run	AGB_{grass} ~ SfM			
	p-value	r^2	RMSE	residual
1	0.163	0.228	84.548	203.680
2	0.028	0.474	87.385	151.420
3	0.033	0.454	98.243	-11.535
4	0.007	0.622	79.474	-196.329
5	0.028	0.474	97.479	-42.163
6	0.048	0.406	97.164	-52.963
7	0.036	0.443	91.368	-123.348
8	0.017	0.533	91.250	141.862
9	0.027	0.479	96.802	59.269
10	0.021	0.507	94.423	-93.822
11	0.027	0.479	97.096	51.493

Appendix IV: Alignment Errors

Table A4.1. Error (RMS) of point cloud alignments. 'Pre' and 'post' refer to data collected before and after AGB removal in the plots. TLS pre scans, TLS post scan 1, and SfM point clouds were all aligned to TLS pre scans. TLS post scans were aligned to TLS post scan 1 after it had been properly aligned to TLS pre scan 1.

Site	TLS pre			TLS post				SfM pre	SfM post
	Scan 2	Scan 3	Scan 4	Scan 1	Scan 2	Scan 3	Scan 4		
1	0.0079	0.0112	0.0172	0.0113	0.0153	0.0169	0.0105	0.0064	0.0107
2	0.0079	0.0118	0.0181	0.0117	0.0172	0.0183	0.0122	0.0107	0.0085
3	0.0130	0.0165	0.0133	0.0219	0.0192	0.0105	0.0169	0.0211	0.0247
4	0.0165	0.0173	0.0170	0.0173	0.0059	0.0150	0.0128	0.0143	0.0155
5	0.0115	0.0154	0.0112	0.0151	0.0077	0.0135	0.0147	0.0139	0.0115
6	0.0126	0.0200	0.0093	0.0105	0.0178	0.0161	0.0138	0.0152	0.0132
7	0.0193	0.0165	0.0041	0.0110	0.0094	0.0133	0.0106	0.0075	0.0205
8	0.0197	0.0199	0.0185	0.0212	0.0115	0.0169	0.0105	0.0192	0.0114
9	0.0126	0.0113	0.0164	0.0141	0.0118	0.0118	0.0023	0.0231	0.0187
10	0.0192	0.0121	0.0190	0.0105	0.0178	0.0161	0.0138	0.0081	0.0153
11	0.0173	0.0083	0.0171	0.0312	0.0115	0.0169	0.0105	0.0125	0.0126